ECOLE DOCTORALE DE PHYSIQUE

ET DE CHIMIE-PHYSIQUE

December 1995

OPTICAL TECHNIQUES FOR THE STUDY OF INTERFACES

Ger Koper
Leiden Institute of Chemistry
Leiden University

1 Electromagnetic theory

1.1 Photons and light

Since the work of J.C. Maxwell in the late eighteen hundreds it is evident that light is most certainly electromagnetic in nature. In classical electrodynamics this leads to the picture of continuous energy transfer by means of electromagnetic *waves*. The modern quantum electrodynamic picture describes the transport of energy in terms of *photons* which are localized quanta of energy. This particle-wave duality will be used here to advantage. For the most part of what follows classical electrodynamics suffices to describe the reflection and refraction of light at surfaces. Ofcourse, quantum electrodynamics needs to be invoked when interaction of light and matter is treated (in section 1.3) but also when the origin of polarization is discussed (in section 1.5).

1.2 Maxwell's equations

The earliest experiments on electromagnetic phenomena, that resulted in for instance Coulomb's law for the force between two electrical charges and Biot-Savart's law for the force between current carying conductors, are now captured by Maxwell's equations supplemented with Lorentz' expression for the force on a moving charge and with an expression for charge conservation.

In Maxwell's theory act an electric field $\boldsymbol{E}$ and a magnetic field $\boldsymbol{B}$. Both are vector fields so that magnitude and direction of the electric field and the magnetic field may vary as a function of time and of position in space. Maxwell's equations in fact summarize the conclusions of a great many of experiments on electromagnetic phenomena. It is exactly at this level where classical electrodynamics is *empirical.*

1.2.1 Faraday's induction law

Faraday discovered that a time-varying magnetic flux, passing through a closed conducting loop, results in the generation of a current through that loop. When the loop is open, one measures the *electromotive force* that drives this current. Mathematically more sophisticated this is written as

$$\oint\limits_{\partial A} \boldsymbol{E} \cdot \boldsymbol{t} \, dr = -\partial_t \int\limits_{A} \boldsymbol{B} \cdot \boldsymbol{n} \, d^2r \tag{1.1a}$$

where A is an open area bounded by the contour ∂A. Here and in the following $\boldsymbol{t}$ denotes the tangential unit vector associated with the line element dr and $\boldsymbol{n}$ the normal unit vector associated with the surface element d^2r. The consequence of this equation is, that a time-varying magnetic field will always have an electric field associated with it.

1.2.2 Gauss' law, electric

Another important observation is named after the German mathematician K.F. Gauss and relates the flux of the electric field through a closed surface ∂V to the total charge in the enclosed volume V. For a space charge distribution $\rho(\boldsymbol{r})$ Gauss' law is written as

$$\oint_{\partial V} \boldsymbol{E} \cdot \boldsymbol{n}\, d^2r = \frac{1}{\epsilon} \int_V \rho\, d^3r. \tag{1.1b}$$

The constant ϵ is known as the electric permittivity and in free space its value is $8.8542 \times 10^{-12}\ \mathrm{C^2N^{-1}m^{-2}}$ in SI units[1]. Other media will be treated in section 1.3.

1.2.3 Gauss' law, magnetic

There is no known magnetic counterpart to the electric charge. Magnetic fields are induced by electric currents, either macroscopic or microscopic as in ferromagnets, and hence the magnetic analog of eq.(1.1b) is

$$\oint_{\partial V} \boldsymbol{B} \cdot \boldsymbol{n}\, d^2r = 0. \tag{1.1c}$$

1.2.4 Ampère's circuital law

As stated before, magnetic fields are generated by electric currents, that is currents of electric charges. This is the great finding of A.M. Ampère. Where Ampère had in mind currents as brought about in conductors by an electric field, Maxwell hypothesized the existence of *displacement currents* as occur between the plates of a capacitor while its charge is varied. Maxwell's restatement of Ampère's circuital law is therefore

$$\oint_{\partial A} \boldsymbol{B} \cdot \boldsymbol{t}\, dr = \mu \int_A (\boldsymbol{j} + \epsilon \partial_t \boldsymbol{E}) \cdot \boldsymbol{n}\, d^2r \tag{1.1d}$$

with $\boldsymbol{j}$ the current density. A is again an open area bounded by the contour ∂A. The quantity μ is called the permeability. For free space its value in SI units is $4\pi \times 10^{-7} \mathrm{Ns^2C^{-2}}$. Other media will be treated in section 1.3.

Just like eq.(1.1a) the above equation has the important consequence, that a time-varying electric field always has a magnetic field associated with it. The two equations together lead to the wave equations that are discussed below.

1.2.5 Maxwell's equations in local form

The set of equations (1.1a...1.1d) can be cast in a local (differential) form which makes them more useful for deriving the wave aspects of the electromagnetic field. This transition can readily be accomplished by making use of two theorems from vector calculus, namely Gauss' divergence theorem

$$\oint_{\partial V} \boldsymbol{F} \cdot \boldsymbol{n}\, d^2r = \int_V \boldsymbol{\nabla} \cdot \boldsymbol{F}\, d^3r \tag{1.2}$$

---

[1] A useful approximation is $\epsilon \approx 1/(36\pi 10^9)$.

and Stokes' theorem

$$\oint_{\partial A} \boldsymbol{F}\cdot\boldsymbol{t}\, dr = \int_{A} (\boldsymbol{\nabla}\times\boldsymbol{F})\cdot\boldsymbol{n}\, d^2r. \tag{1.3}$$

with $\boldsymbol{F}$ an arbitrary vector field. The result is

$$\begin{aligned} \boldsymbol{\nabla}\times\boldsymbol{E} &= -\partial_t\boldsymbol{B} && (1.4a)\\ \boldsymbol{\nabla}\cdot\boldsymbol{E} &= \rho/\epsilon && (1.4b)\\ \boldsymbol{\nabla}\cdot\boldsymbol{B} &= 0 && (1.4c)\\ \boldsymbol{\nabla}\times\boldsymbol{B} &= \mu(\boldsymbol{j}+\epsilon\,\partial_t\boldsymbol{E}) && (1.4d) \end{aligned}$$

In free space, where there are no charges ($\rho = 0$) and where there are no currents ($\boldsymbol{j} = \boldsymbol{0}$), the combination of eq.(1.4a) and eq.(1.4d) immediately leads to two extremely concise vector equations

$$\nabla^2\boldsymbol{E} = \epsilon\mu\partial_t^2\boldsymbol{E} \tag{1.5a}$$

and

$$\nabla^2\boldsymbol{B} = \epsilon\mu\partial_t^2\boldsymbol{B}. \tag{1.5b}$$

These equations are the *wave equations* and they predict solutions in the form of electromagnetic waves with a velocity $c = 1/\sqrt{\epsilon\mu}$. It was exactly this prediction, which was experimentally verified by A.H.L. Fizeau, that made Maxwell's formulation of classical electrodynamics one of the great intellectual triumphs of all times.

1.2.6 General solutions

The general solution of Maxwell's equations in the presence of charges and electric currents can easily be formulated in terms of an electric potential $\varphi(\boldsymbol{r},t)$ and a magnetic vector potential $\boldsymbol{A}(\boldsymbol{r},t)$ such that[2]

$$\boldsymbol{E} = -\boldsymbol{\nabla}\varphi - \partial_t\boldsymbol{A}, \tag{1.6a}$$

and

$$\boldsymbol{B} = \boldsymbol{\nabla}\times\boldsymbol{A} \tag{1.6b}$$

The solution of Maxwell's equations is then written as

$$\begin{aligned} \varphi(\boldsymbol{r},t) &= \int \frac{1}{4\pi\epsilon|\boldsymbol{r}-\boldsymbol{r}'|}\rho\left(\boldsymbol{r}',t-\frac{|\boldsymbol{r}-\boldsymbol{r}'|}{c}\right)\, d^3r' && (1.7a)\\ \boldsymbol{A}(\boldsymbol{r},t) &= \int \frac{1}{4\pi\mu|\boldsymbol{r}-\boldsymbol{r}'|}\boldsymbol{j}\left(\boldsymbol{r}',t-\frac{|\boldsymbol{r}-\boldsymbol{r}'|}{c}\right)\, d^3r'. && (1.7b) \end{aligned}$$

The time argument in the charge and current contains a term $|\boldsymbol{r}-\boldsymbol{r}'|/c$ which accounts for the retardation: a disturbance at some location $\boldsymbol{r}'$ takes some time, even as it travels at the speed of light, to reach the position $\boldsymbol{r}$. When retardation effects are not important this term can be neglected and Maxwell's equations are treated in the *static limit.*

---

[2] There is some freedom in the choice of potentials but that is not of relevance here.

1.2.7 Multipole expansion

The simplest electrostatic problem to consider is the case of a single charge located in the origin

$$\rho_1(\boldsymbol{r}) = q\delta(\boldsymbol{r}). \tag{1.8}$$

The electrostatic potential for this case is the well-known Coulomb potential

$$\varphi_1(\boldsymbol{r}) = \frac{q}{4\pi\epsilon r}. \tag{1.9}$$

The next simplest case is the *physical* dipole that consists of two opposite charges at a given seperation

$$\rho_2(\boldsymbol{r}) = q\left(\delta(\boldsymbol{r} - \frac{\boldsymbol{d}}{2}) - \delta(\boldsymbol{r} + \frac{\boldsymbol{d}}{2})\right) \tag{1.10}$$

with the electrostatic potential

$$\varphi_2(\boldsymbol{r}) = \frac{q}{4\pi\epsilon}\left(\frac{1}{|\boldsymbol{r} - \frac{\boldsymbol{d}}{2}|} - \frac{1}{|\boldsymbol{r} + \frac{\boldsymbol{d}}{2}|}\right). \tag{1.11}$$

The transition to a mathematical or *point dipole* occurs when taking the limit $d \to 0$ while keeping the dipole moment $\boldsymbol{p} = q\boldsymbol{d}$ constant:

$$\varphi_2(\boldsymbol{r}) \simeq \frac{1}{4\pi\epsilon}\frac{\boldsymbol{p}\cdot\boldsymbol{r}}{r^3} \quad \text{for} \quad d \to 0 \quad \text{while} \quad p = qd \quad \text{constant.} \tag{1.12}$$

For what follows it is important to note, that the above potential can also be written as the derivative of the *electrostatic propagator*

$$\varphi_2(\boldsymbol{r}) = \boldsymbol{p}\cdot\boldsymbol{\nabla}\frac{1}{4\pi\epsilon r}. \tag{1.13}$$

Let us now consider an arbitrary charge distribution $\rho(\boldsymbol{r})$ inside a volume V around the origin and suppose that we wish to know the electrostatic potential in some far-away point $\boldsymbol{r}$. By expanding the propagator in the electrostatic potential

$$\varphi(\boldsymbol{r}) = \int\limits_V \frac{1}{4\pi\epsilon|\boldsymbol{r} - \boldsymbol{r}'|}\rho(\boldsymbol{r}')d\boldsymbol{r}'. \tag{1.14}$$

in a Taylor series,

$$\frac{1}{|\boldsymbol{r} - \boldsymbol{r}'|} = \frac{1}{r} + \boldsymbol{r}'\cdot\boldsymbol{\nabla}\frac{1}{r} + \frac{1}{2!}\boldsymbol{r}'\boldsymbol{r}' : \boldsymbol{\nabla}\boldsymbol{\nabla}\frac{1}{r} + \ldots, \tag{1.15}$$

the *multipole expansion* of the charge distribution is obtained[3]

$$\varphi(\boldsymbol{r}) = \frac{1}{4\pi\epsilon}\left\{\frac{q}{r} + \boldsymbol{p}\cdot\boldsymbol{\nabla}\frac{1}{r} + \boldsymbol{Q} : \boldsymbol{\nabla}\boldsymbol{\nabla}\frac{1}{r} + \ldots\right\} \tag{1.16}$$

---

[3] Note that values of the multipole coefficients depend on the choice of the coordinate system except the lowest order non-zero coefficient.

with the total charge

$$q \equiv \int_V \rho(\boldsymbol{r}')d\boldsymbol{r}', \tag{1.17a}$$

the total dipole moment

$$\boldsymbol{p} \equiv \int_V \boldsymbol{r}'\rho(\boldsymbol{r}')d\boldsymbol{r}', \tag{1.17b}$$

the total quadrupole moment

$$\boldsymbol{Q} \equiv \int_V \boldsymbol{r}'\boldsymbol{r}'\rho(\boldsymbol{r}')d\boldsymbol{r}', \tag{1.17c}$$

etc. Each term in this multipole expansion is a factor r^{-2} weaker than its predecessor. The conclusion of this analysis is therefore, that the lowest order non-zero multipole moment gives the dominant contribution to the electrostatic potential.

1.3 Light and matter

Although molecules are neutral a great many of them have a non-symmetrical charge distribution which gives rise to a *permanent dipole moment.* The water molecule for instance has a center of gravity of the positive charge that is more on the hydrogen side of the molecule whereas the center of gravity of the negative charge is more on the oxygen side of the molecule. It therefore carries a permanent dipole moment of 6.17×10^{-30} Cm. On the other hand the oxygen molecule is nicely symmetric and carries no permanent dipole[4]. In the absence of an electric field thermal agitation keeps the molecule randomly oriented so that there is a vanishing (time-) averaged dipole moment. With a (not too large) applied electric field E there is a tendency to line up along the field in the configuration of lowest energy leading to a nonvanishing average dipole moment

$$\langle \boldsymbol{p} \rangle \simeq \frac{p_0^2}{3k_BT}\boldsymbol{E} \tag{1.18}$$

with p_0 the permanent dipole moment, k_B=1.38×10^{-23} J/K the Boltzmann constant and T absolute temperature, see exercise 1.1.

The charges in a molecule are mobile and hence, when an electric field is applied, the electronic and even the atomic structure of the molecule is distorted and this, in turn, gives rise to an *induced dipole moment*

$$p = \alpha E + \beta E^2 + \ldots. \tag{1.19}$$

For not too large electric fields the induced dipole moment is linear in the electric field. The proportionality constant α is called the *polarizability* of the molecule and it is mainly of electronic origin. For higher electric fields the induced dipole moment is no longer linear in the applied field and this can be accounted for by for instance the *hyperpolarizability* β (see eq.(1.19)).

---

[4] Dipole moments of molecules, bonds, and molecular groups are sometimes expressed in *Debije units*: $1D = 3.336 \times 10^{-30}$Cm.

1.3.1 Polarization

Consider a capacitor consisting of two flat plates that have charges per unit area of $+\sigma$ and $-\sigma$ respectively. In the absence of matter between the plates the magnitude of the electric field between the plates is equal to σ/ϵ_0 where the dielectric permittivity of vacuum is denoted by ϵ_0. When a (non-conducting) material is inserted between the plates Faraday already noticed that the magnitude of the electric field drops. For this situation one still writes for the magnitude of the electric field σ/ϵ but now with a dielectric permittivity $\epsilon > \epsilon_0$. The reason for the drop in the electric field is that the electric field effectively induces dipoles in the *dielectric*, either by aligning the molecular permanent dipoles or by inducing molecular dipole moments. For not too large electric fields the induced *polarization* is linear in the electric field

$$\boldsymbol{P} = \epsilon_o \chi \boldsymbol{E}, \tag{1.20}$$

where χ is called the *susceptibility* of the dielectric. The magnitude of the electric field between the plates of the capacitor can still be related to both the surface charge and the polarization by

$$E = \frac{\sigma - P}{\epsilon_0} \tag{1.21}$$

from which one derives $\epsilon = \epsilon_0(1+\chi)$. Note that the polarization acts as a surface charge, see exercise 1.2. The quantity $\epsilon_r = \epsilon/\epsilon_0 = 1+\chi$ is called the *relative dielectric permittivity* of the dielectric.

The relation between the dielectric permittivity and the molecular polarizability of a dielectric is given by the Clausius-Mossotti relation

$$\frac{\epsilon - \epsilon_0}{\epsilon + 2\epsilon_0} = \frac{\rho}{3\epsilon_0}\left\{\alpha + \frac{p_0^2}{3k_B T}\right\} \tag{1.22}$$

with ρ the molecular density of the dielectric, see exercise 1.3. This relation is derived under the assumption that the molecules in the dielectric are identical and uncorrelated. It is trivially extended to the case of more than one species of molecules. Correlations are usually taken into account by means of a *virial expansion*. In particular for fluids (gases and simple liquids) the Clausius-Mossotti relation fits experimental data quite satisfactory.

1.3.2 Dispersion

Up till now only static electric fields were considered. For time-varying fields of low frequency the above relations still hold; this is the *quasi-static regime*. For higher frequencies the molecular susceptibility is frequency-dependent and this phenomenon is called *dispersion*. There are two distinct mechanisms that give rise to dispersion and both can be captured by the same formula[5]:

$$\alpha(\omega) = \frac{\alpha_0 \omega_0^2}{\omega_0^2 + \mathrm{i}\omega\omega_0\gamma - \omega^2} \tag{1.23}$$

---

[5] In electromagnetism it is customary to use Fourier-transformed quantities. Here ω is to be regarded as the frequency of the applied electric field.

with α_0 the low-frequency (static) limit of the polarizability.

A permanent dipole rotates to follow the instantaneous direction of the electric field. Clearly, the rotational friction ξ_r plays a dominant role but also the moment of inertia I of the molecule comes into play. By substituting $\alpha_0 = p_0^2/3k_BT$, $\gamma = \xi_r/\sqrt{2k_BTI}$, and $\omega_0^2 = 2k_BT/I$ the response function eq.(1.23) accounts for this phenomenon. In many situations $\omega/\omega_0 \ll 1$ and eq.(1.23) can be approximated by the well-known Debije relaxation formula

$$\alpha(\omega) = \frac{\alpha_0}{1 + \mathrm{i}\omega\tau} \tag{1.24}$$

with the rotation correlation time $\tau = \gamma/\omega_0 = \xi_r/2k_BT$. The polarizability is a complex number. The real part is *in phase* with the incident field and the imaginary part is *out of phase* with the incident field. The imaginary part reflects the energy absorption: the rotational friction of the molecule causes electromagnetic energy to be transferred to the surrounding molecules.

Each charge in a molecule can be considered as harmonically bound to its rest position. The restoring force is then proportional to ω_0^2 and the damping of the motion is measured by γ. In principle the calculation of α_0, ω_0, and γ is a quantum mechanical problem but the thus desribed *Sellmeier damped-oscillator model* provides for an adequate picture, see exercise 1.4.

In general there are more than one contribution to the dispersion and one writes for the polarizability

$$\alpha(\omega) = \sum_k \frac{\alpha_k \omega_k^2}{\omega_k^2 + \mathrm{i}\omega\omega_k\gamma_k - \omega^2}. \tag{1.25}$$

Typically there are three dispersion regimes: For low frequencies (static limit) the *orientational polarization*, the polarization arising from the permanent dipole moments, is the most important. Since the rotation correlation time of a molecule is typically of the order of 1 ps this contribution vanishes in the microwave regime ($10^9 \ldots 10^{11}$ Hz). At the infrared frequencies ($10^{11} \ldots 10^{14}$ Hz) the *distortion polarization* vanishes. This polarization arises from distortions in the positions of the nuclei due to the electric field. At even higher frequencies only the electrons can still participate. At each absorption frequency, typically in the visible or ultraviolet regime, another electronic term in the polarizability vanishes. A typical graph of the polarizability as a function of frequency is given in fig. 1.1.

1.3.3 Magnetization

For the magnetic properties of matter a presentation similar to the one in section 1.3.1 can be given. In practice, however, it is hardly ever necessary to deal with magnetic properties of matter which is reflected by the fact that the *relative permeability* for most materials is equal to one.

1.3.4 Refractive index

As stated in section 1.2.5 electromagnetic waves, like light, have a velocity $v = 1/\sqrt{\epsilon\mu}$. This velocity is highest in vacuum, where it is approximately equal to 3×10^8 m/s.

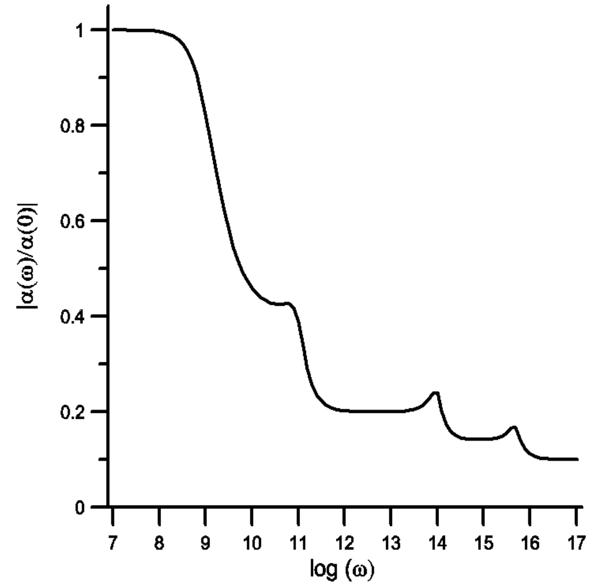

Fig. 1.1. Typical graph of polarizability versus frequency.

In any other material this velocity is smaller and the ratio of the speed of an electromagnetic wave in vacuum to that in matter is the *absolute index of refraction* of the material and it is given by

$$n = \sqrt{\frac{\epsilon\mu}{\epsilon_0\mu_0}}. \tag{1.26}$$

Since for most materials the relative permeability is equal to 1 one has from eq.(1.26) for the relative dielectric permittivity $\epsilon_r = n^2$. Substituting this in the Clausius-Mossotti relation (1.22) with the polarizability given by eq.(1.25) yields the *Lorentz-Lorenz* relation:

$$\frac{n^2-1}{n^2+2} = \frac{\rho}{3\epsilon_0}\alpha \tag{1.27}$$

This relation shows that, for non-magnetic systems, the refractive index is frequency-dependent exactly in the same way as the dielectric permittivity.

1.4 Maxwell's equations in isotropic media

In many materials, like most dielectrics, the induced polarization is indeed linear in the electric field so that eq.(1.20) holds. In a similar way one often has a magnetization $\boldsymbol{M}$ linear in the magnetic field. Both statements are ofcourse only true for a limited range of field strengths. For optical experiments this is almost always the case. It was for this reason that Maxwell used, besides the electric field $\boldsymbol{E}$ and the magnetic field $\boldsymbol{B}$, the *electric displacement* $\boldsymbol{D} = \epsilon_0\boldsymbol{E}+\boldsymbol{P}$ and the *magnetic induction* $\boldsymbol{H} = \boldsymbol{B}/\mu_0 - \boldsymbol{M}$[6].

---

[6] Sometimes one defines $\boldsymbol{H}' = \boldsymbol{B} - \mu_0\boldsymbol{M}$ such that $\boldsymbol{H}'$ and $\boldsymbol{B}$ have the same units.

The eqs.(1.4a...1.4d) with the above mentioned substitutions then take a very simple form:

$$
\begin{aligned}
\boldsymbol{\nabla} \times \boldsymbol{E} &= -\partial_t \boldsymbol{B} && (1.28a)\\
\boldsymbol{\nabla} \cdot \boldsymbol{D} &= \rho' && (1.28b)\\
\boldsymbol{\nabla} \cdot \boldsymbol{B} &= 0 && (1.28c)\\
\boldsymbol{\nabla} \times \boldsymbol{H} &= \boldsymbol{j}' + \partial_t \boldsymbol{D} && (1.28d)
\end{aligned}
$$

which are to be used with the *constitutive relations*

$$\boldsymbol{D} = \epsilon \boldsymbol{E}, \tag{1.29a}$$

and

$$\boldsymbol{H} = \boldsymbol{B}/\mu. \tag{1.29b}$$

The charge density ρ' and current density $\boldsymbol{j}'$ are the charges and currents that are introduced into the medium. In free space the dielectric permittivity is ϵ_0 and the magnetic permeability is μ_0. Substituting these for ϵ and μ in eqs.(1.28a...1.28d) and in the constitutive equations (1.29a,1.29b) yields Maxwell's equations in local form (1.4a...1.4d).

1.5 Polarized light

One of the simplest solutions of the wave equation (1.5a) is the *monochromatic plane wave.* The electric field of such a plane wave is given as

$$\boldsymbol{E}(\boldsymbol{r},t) = E_0 \boldsymbol{e} \exp\{\mathrm{i}(\omega t - \boldsymbol{k} \cdot \boldsymbol{r})\} \tag{1.30}$$

where it is understood that, in order to obtain a physical field, the real part has to be taken[7]. E_0 is the amplitude of the electric field and $\boldsymbol{e}$ is a unit vector that determines the *polarization* of the light. Light is a *transverse* wave which means that the electric field varies in a plane perpendicular to the *propagation vector* $\boldsymbol{k}$, i.e. $\boldsymbol{e} \cdot \boldsymbol{k} = 0$. The magnitude of the propagation vector is the *propagation number* $k = 2\pi/\lambda$ with λ the *wavelength* in the medium. It is related to the *frequency* ω by the equation $k = \omega/v$ where v is the wave velocity in the medium. It is customary to relate to the speed c of light and the wavelength λ_0 in vacuum:

$$k = \frac{2\pi n}{\lambda_0} = \frac{\omega n}{c} \tag{1.31}$$

with n the refractive index of the medium.

The plane wave does not occur in nature but it is a convenient device for calculations because any physical wave can be represented as a sum of plane waves. Two types of physical waves need particular attention. The one is the monochromatic *spherical wave*

---

[7] The magnetic field is always perpendicular to both the electric field and the propagation vector and, for nonmagnetic material, trivially related to the electric field. Therefore it is customary only to refer to the electric field.

$$E(\boldsymbol{r},t) = E_0 \frac{e^{\mathrm{i}(\omega t - kr)}}{kr} \tag{1.32}$$

which is a good description for the light emitted by a point source. The other is the *Gaussian beam* which is a good approximation for a (single mode) laser beam[8]. A beam travelling in the z-direction it is represented by

$$E(\boldsymbol{r},t) = E_0 \sqrt{\frac{2}{\pi}} \frac{e^{\mathrm{i}(\omega t - kz)-(x^2+y^2)/w^2(z)}}{w^2(z)} \tag{1.33}$$

with the position dependent spot size $w(z)$ which, for z sufficiently large, is given by

$$w(z) \simeq \frac{\lambda z}{\pi w_0} \tag{1.34}$$

The *waist* w_0 is a design parameter of the laser.

1.5.1 The nature of polarized light

The *plane of vibration*, that is the plane in which the electric field varies, is perpendicular to the propagation vector. An arbitrary coherent wave can therefore always be decomposed in two orthogonally vibrating component waves[9]. Assuming the propagation vector along the positive z-axis of a Cartesian coordinate system, these component waves can be represented as

$$\begin{aligned} \boldsymbol{E}_x &= E_{0,x}\boldsymbol{e}_x e^{\mathrm{i}(\omega t - kz)} \\ \boldsymbol{E}_y &= E_{0,y}\boldsymbol{e}_y e^{\mathrm{i}(\omega t - kz + \varphi)} \end{aligned} \tag{1.35}$$

where $\boldsymbol{e}_x$ and $\boldsymbol{e}_y$ are the unit vectors in the positive x-direction and y-direction respectively. $E_{0,x}$ and $E_{0,y}$ are the amplitudes of the electric field components and φ is the phase difference. Only phase differences between $-\pi$ and π are relevant.

Each of the components represents a *linearly polarized* wave. For $\varphi = 0$ the two components are *in phase* and the resultant of the two components is also linearly polarized because the amplitude $E_{0,x}\boldsymbol{e}_x + E_{0,y}\boldsymbol{e}_y$ is fixed. One could equally well have chosen the x-axis along the resultant and then the y-component would have zero amplitude. For $\varphi = \pi/2$ and equal amplitudes $E_{0,x} = E_{0,y} = E_0$ the resultant wave is *left circularly polarized*: the (real part of) the resultant field is written as

$$\boldsymbol{E} = E_0 \left\{\boldsymbol{e}_x \cos(\omega t - kz) + \boldsymbol{e}_y \sin(\omega t - kz)\right\} \tag{1.36}$$

and rotates counterclockwise in the plane of vibration, thus describing a circle. For $\varphi = -\pi/2$ the wave is *right circularly polarized.* For arbitrary φ the light is said to be *elliptically polarized*, see fig. 1.2.

---

[8] see A.E. Siegman, *Lasers*, Oxford University Press, Oxford, chapter 17.

[9] Coherent light consists of components that have a fixed phase difference in time. Natural light is incoherent and in practice light is only partially coherent. For most practical considerations laser light can be considered to be coherent.

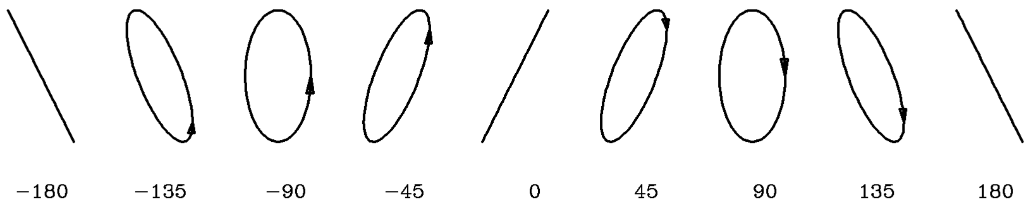

Fig. 1.2. Various polarization states corresponding to specific values of φ (in degrees).

The linear polarized wave seems to be the most straightforward from a mathematical point of view. Circular polarized light on the other hand seems to be a rather peculiar notion that can best be considered as the resultant of two linear polarized waves with $\pi/2$ phase difference. From a physical point of view, however, the opposite is the case! The polarization of light originates from the angular momentum of the photons: because of the quantized nature of angular momentum (a photon is a spin 1 particle) photons can be considered as wave-packets which are either right-circular or left-circular polarized. Now linear polarized light appears to be the artifact that consists of a photon current, half of the photons in the left-circular state and the other half in the right-circular state!

1.5.2 Jones notation

As discussed before the plane of vibration is determined by two unit vectors. For polarized light it therefore suffices to discuss the projection of the electric field in the plane of vibration. This reduces the number of relevant components of the vector to 2 and such vectors are called *Jones vectors* after the american physicist R. Clark Jones who invented the notation in 1941[10].

To give an example for light that travels along the positive z-axis, the electric field vector is written as

$$\boldsymbol{E} = \begin{pmatrix} E_{0,x}e^{\mathrm{i}\varphi_x} \\ E_{0,y}e^{\mathrm{i}\varphi_y} \\ 0 \end{pmatrix} e^{\mathrm{i}(\omega t - kz)} \tag{1.37}$$

and the Jones vector is

$$\boldsymbol{E} = \begin{pmatrix} E_{0,x}e^{\mathrm{i}\varphi_x} \\ E_{0,y}e^{\mathrm{i}\varphi_y} \end{pmatrix} \tag{1.38}$$

Each optical component has its own Jones matrix T_k and when light with Jones vector $\boldsymbol{E}_i$ passes through a sequence of these components the outcoming light has the Jones vector $\boldsymbol{E}_o$ given by

$$\boldsymbol{E}_o = T_n T_{n-1} \ldots T_2 T_1 \boldsymbol{E}_i \tag{1.39}$$

---

[10] For unpolarized or partially polarized light the Jones notation cannot be used. One then uses the much more involved Müller notation that will not be further discussed here.

where standard matrix multiplication is implied, see exercise 1.5.

A horizontal *linear polarizer* has Jones matrix

$$T_0 = \begin{pmatrix} 1 & 0 \\ 0 & 0 \end{pmatrix} \tag{1.40}$$

and, using the matrix for rotation through an angle α

$$R_\alpha = \begin{pmatrix} \cos\alpha & \sin\alpha \\ -\sin\alpha & \cos\alpha \end{pmatrix} \tag{1.41}$$

the Jones matrix for a linear polarizer of which the axis makes an angle α with the horizontal is calculated as

$$T_\alpha = R_{-\alpha} T_0 R_\alpha = \begin{pmatrix} \cos^2\alpha & \cos\alpha\sin\alpha \\ \cos\alpha\sin\alpha & \sin^2\alpha \end{pmatrix} \tag{1.42}$$

Another useful optical component is a *retarder* that effects a phase difference δ between its *fast* and *slow* axis

$$T_{\delta,0} = \begin{pmatrix} e^{\mathrm{i}\delta/2} & 0 \\ 0 & e^{-\mathrm{i}\delta/2} \end{pmatrix}. \tag{1.43}$$

Retarders can be used to change for instance linear polarized light into circular polarized light and back. Although it is not often done it is possible to include polarization-dependent absorption in the Jones notation.

Exercises

1.1 The energy of a dipole moment $\boldsymbol{p}_0$ in an electric field $\boldsymbol{E}$ is equal to $u = -\boldsymbol{p}_0 \cdot \boldsymbol{E}$. Use the Boltzmann weight $\exp(-\beta u)$ to derive

$$\langle \boldsymbol{p} \rangle \simeq p_0 \frac{\beta p_0 E \sinh \beta p_0 E - \cosh \beta p_0 E}{\beta p_0 E \cosh \beta p_0 E} \boldsymbol{E}$$

with $\beta \equiv 1/k_B T$ (Choose the z-axis of the coordinate system along $\boldsymbol{E}$). Subsequently show that for small relative energies $\beta p_0 E$ this leads to eq.(1.18).

1.2 Consider a parallel-plate capacitor with surface charge σ. Calling the spacing between the plates d the voltage across the capacitor is given by the integral of the electric field over the distance between the plates. This yields

$$V = \frac{\sigma d}{\epsilon_0}$$

and hence the capacitance is

$$C = \frac{Q}{V} = \frac{\epsilon_0 A}{d}.$$

where the plate area is taken to be A.
(1) show that when a conductor of thickness $b < d$ is inserted between the plates, the induced surface charge in the conductor leads to an increased capacitance

$$C = \frac{\epsilon_0 A}{d(1 - b/d)}$$

(2) when a dielectric is inserted the capacitance increases also due to an induced surface charge. This *polarization charge* arises from a net displacement δ of the positive molecular charges with respect to the negative charges, see fig.1.3. Calling ρ the positive (or negative) charge density and q the elementary charge, the induced dipole moment is $P = \rho q \delta$. Argue, using fig.1.3, that the polarization charge is equal to P and derive

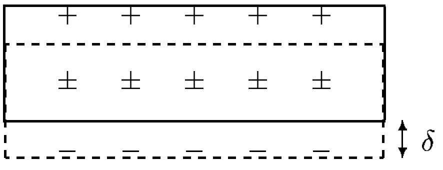

Fig. 1.3. A dielectric slab in a uniform field.

$$C = \frac{\epsilon_0(1 + \chi)A}{d}$$

using eq.(1.20).

1.3 When an isotropic dielectric is placed in a homogeneous electric field E the molecules in the dielectric experience not the field E but a field that is modified by the presence of the other molecules. Let the polarization in the dielectric be P. Imagine we remove one of the molecules from the dielectric. What is left is a hole and for the electric field in the hole one derives[11]

$$E_{\text{hole}} = E + \frac{P}{3\epsilon_0}.$$

The induced dipole in the molecule is then proportional to this field with polarizability α. For a density of ρ molecules per unit volume one has

$$P = \rho\alpha\left(E + \frac{P}{3\epsilon_0}\right).$$

Use this to derive eq.(1.22).

---

[11] see R.P. Feynman et al, *Lectures on Physics* II, sec.11.4, Addison-Wesley, Reading Mass., 1964.

1.4 Consider an electron, mass m and charge q, harmonically bound (force constant k_0) to a nucleus (at rest) in an oscillating electric field $E(t) = E_0 e^{\mathrm{i}\omega t}$. Newton's law gives the equation of motion of the electron in terms of the displacement x of the electron from the nucleus

$$m\partial_t^2 x = -k_0 x + qE(t)$$

The polarization of this simple system is $P(t) = qx(t)$.
(1) Show that for frequencies $\omega \neq \omega_0$

$$P(t) = \frac{\alpha_0 \omega_0^2}{\omega_0^2 - \omega^2} E_0 e^{\mathrm{i}\omega t},$$

where $\omega_0^2 = k_0/m$ and $\alpha_0 \omega_0^2 = q/m$.
(2) The response at the resonance frequency ω_0 is undetermined. Include a friction force $-\xi\partial_t x$ to overcome this problem and derive eq.(1.23).
(3) Show that in the neighbourbood of the resonance frequency

$$\partial_t^2 x = \frac{qE_0}{2m\omega_0} \frac{Q}{(\omega - \omega_0)^2 + Q^2}$$

where $Q = \xi/2m$. The plot of $\partial_t^2 x$ versus frequency is called a *Lorentzian distribution.* It is commonly used to represent the shape of the lines in an absorption spectrum.

1.5 Unpolarized light passes through a sequence of two linear polarizers of which the axes make an angle α with one another. Derive an expression for the transmitted light intensity as a function of the angle α; this is Malus' law.

2 Reflection at interfaces

2.1 Geometrical considerations

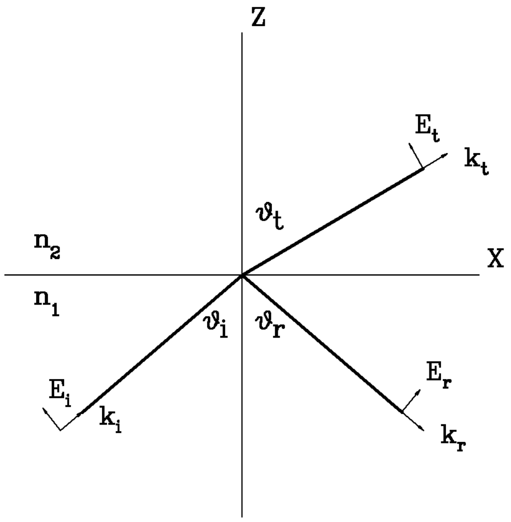

Fig. 2.1. Reflection and transmission of p-polarized light at a planar interface between two semi-infinite homogeneous optically isotropic media.

Consider, with reference to fig. 2.1, the oblique reflection and transmission of a plane wave at the planar interface between two semi-infinite homogeneous optically isotropic media 1 and 2 with (complex) indices of refraction n_1 and n_2, respectively. It is assumed that the change in index of refraction is abrupt across the interface, i.e. is a step function of the coordinate perpendicular to the interface. The wave incident in medium 1 gives rise to a *reflected* wave in the same medium and a *transmitted*, or more appropriately *refracted* wave, in medium 2. The *angle of incidence* θ_i, the *angle of refraction* θ_t, and the *angle of reflection* θ_r are measured from the direction of the normal to the interface. The total fields inside media 1 and 2 obey Maxwell's equations (cf. eqs. (1.28a ... 1.28d)) and the boundary conditions at the interface. For the boundary conditions to be satisfied

- the directions of propagation of the incident, reflected, and transmitted waves must all lie in the *plane of incidence* determined by the normal of the interface and the direction of propagation of the incident beam,

- the angle of incidence must equal the angle of reflection, i.e.

  $$\theta_i = \theta_r, \tag{2.1}$$

  and

- the angles of incidence and refraction must be related by *Snell's law*:

  $$n_1 \sin\theta_i = n_2 \sin\theta_t. \tag{2.2}$$

If media 1 and 2 are transparent, so that n_1 and n_2 are both real numbers, the angle θ_t is real. However, when either one or both media are absorbing, the angle θ_t becomes, in general, more complex and eq. (2.2) holds formally but the physical picture is more complicated.

The law of reflection (2.1) is much more fundamental than it appears from this introduction. It can be derived easily by considering the interference of wavelets originating from the scatterers in the medium[1]. Consider as an example a homogeneous distribution of scatterers in a plane, see fig. 2.2. A plane wave is incident on this plane with angle θ_i. In all but one direction the spherical waves emerging from the scatterers interfere destructively. The one direction where there is constructive interference is in the plane of incidence and makes an angle θ_i with the normal to the interface (see exercise 2.1).

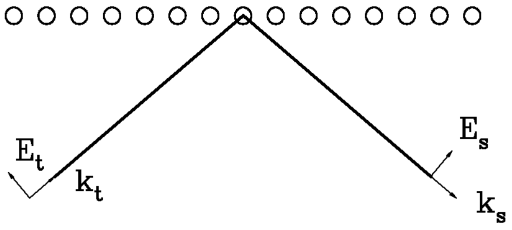

Fig. 2.2. Assembly of scatterers in a plane obeying the law of reflection.

2.2 The Fresnel equations

For a given amplitude and polarization of the incident wave, the amplitude and polarization of the reflected and transmitted waves can be determined from the continuity of the tangential components of the electric and magnetic field across the interface. It can be shown that when the incident wave is linearly polarized with the electric field *parallel* to the plane of incidence (*p-waves*), the reflected and transmitted waves are also linearly polarized with their electric field vectors parallel to the plane of incidence. Likewise, when the incident wave is linearly polarized *perpendicular* to the plane of incidence (*s-waves*[2]), the reflected and transmitted waves are also linearly polarized perpendicular to the same plane.

---

[1] For crystals the phenomenon is known as *Bragg reflection.*

[2] The letter s originates from the German word *senkrecht* for perpendicular.

In terms of Jones notation (cf. section 1.5.2) the transfer matrix for reflection or transmission has two eigenvectors corresponding to linear polarized light with electric field parallel (p) and perpendicular (s) to the plane of incidence. This is, however, only true if both media are optically isotropic as is assumed in what follows. The Jones matrix for reflection (transmission) is, in general, not energy conservative since part of the energy is transmitted (reflected). Let (E_{ip}, E_{is}), (E_{rp}, E_{rs}), and (E_{tp}, E_{ts}) represent the Jones vectors for incident, reflected and transmitted light respectively, then the Jones matrix for reflection is

$$\mathcal{R} = \begin{pmatrix} r_p & 0 \\ 0 & r_s \end{pmatrix} \tag{2.3a}$$

and for transmission it is

$$\mathcal{T} = \begin{pmatrix} t_p & 0 \\ 0 & t_s \end{pmatrix}. \tag{2.3b}$$

The reflection and transmission amplitude ratios, due to Augustin Jean Fresnel (1788 – 1827), can be derived by matching the tangential electric and magnetic field across the interface. They are[3]

$$r_p = \frac{n_2 \cos\theta_i - n_1 \cos\theta_t}{n_2 \cos\theta_i + n_1 \cos\theta_t} \tag{2.4a}$$

$$r_s = \frac{n_1 \cos\theta_i - n_2 \cos\theta_t}{n_1 \cos\theta_i + n_2 \cos\theta_t} \tag{2.4b}$$

$$t_p = \frac{2n_1 \cos\theta_i}{n_2 \cos\theta_i + n_1 \cos\theta_t} \tag{2.4c}$$

$$t_s = \frac{2n_1 \cos\theta_i}{n_1 \cos\theta_i + n_2 \cos\theta_t} \tag{2.4d}$$

The incidence angle θ_i and the angle of transmission θ_t are related by Snell's law (2.2).

The reflective properties of interfaces are described either by the reflectivities $R_p = |r_p|^2$ and $R_s = |r_s|^2$ for p-waves and s-waves respectively, or by the ellipsometric angles ψ and Δ determining the (complex) ratio

$$\frac{r_p}{r_s} = \tan\psi e^{\mathrm{i}\Delta} \tag{2.5}$$

In figure 2.3 two examples of reflectivities are given, one for the air/glass and the other for the glass/air interface. The marked difference between the two is the angle of total reflectance for the glass/air interface which is absent for the air/glass interface. The existence of such an angle can be deduced from Snell's law (2.2): upon transition from a dense into a less dense medium the refractive index jumps to a smaller value and hence the angle of propagation with the normal increases. Increasing the angle of incidence, the angle of refraction in the less dense medium reaches 90 degrees sooner than does the angle of incidence. Beyond this angle of total reflection no light is refracted and all is reflected. In actual fact, some electromagnetic field is still

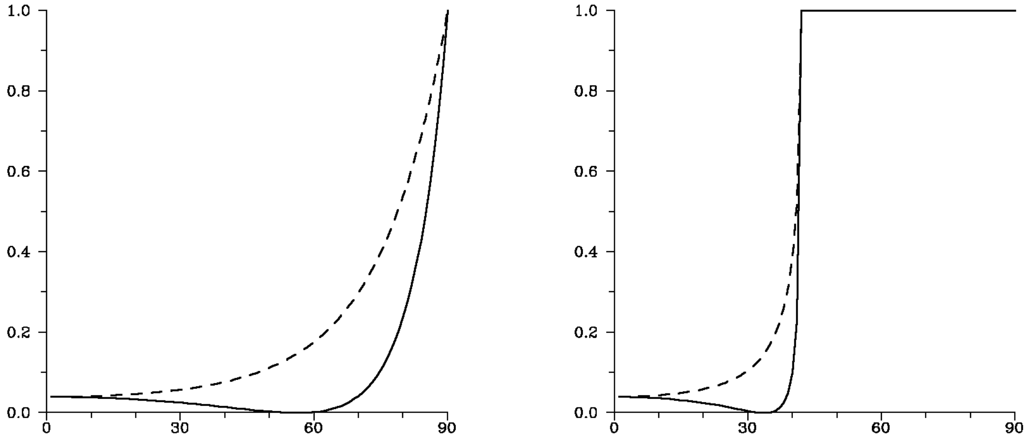

Fig. 2.3. Reflectivities (drawn lines for p-wave and dashed lines for s-wave) for the air/glass (*left*) and the glass/air (*right*) interface as a function of angle of incidence.

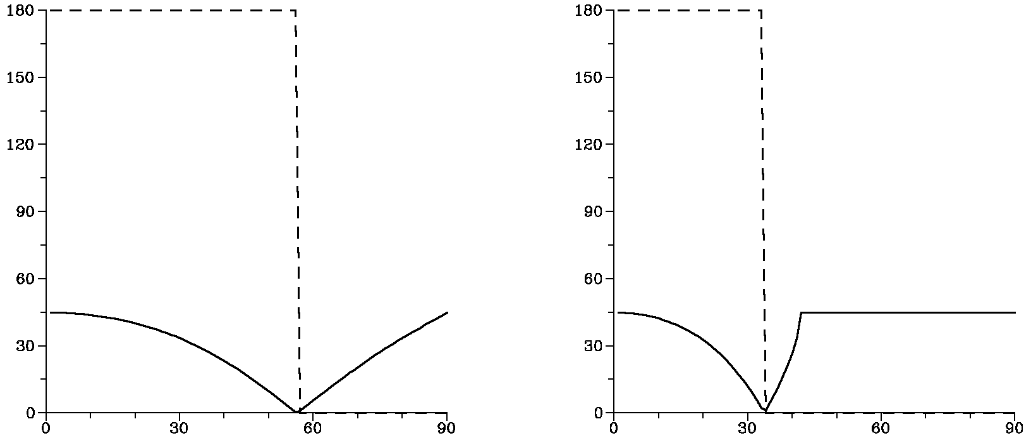

Fig. 2.4. Ellipsometric angles (drawn lines for ψ and dashed lines for Δ) for the air/glass (*left*) and the glass/air (*right*) interface as a function of angle of incidence.

present near the interface in the other medium, this is called the *evanescent wave.* At normal incidence ($\theta_i = 0$) there is no distinction between p-waves and s-waves and consequently there can be no difference between the normal reflectivities. The p-wave reflectivity passes through a minimum, $R_p = 0$, at the *Brewster angle* or *polarizing angle.* Inspection of eq. (2.4a), with the help of Snell's law (2.2), shows that this angle is given by

$$\theta_B = \arctan\left(\frac{n_2}{n_1}\right). \tag{2.6}$$

At this angle the incidence wave is *totally refracted* into the second medium. Also, the p-wave amplitude reflection coefficient (2.4a) changes sign at this angle which causes the ellipsometric angle Δ to jump 180 degrees, see fig. 2.4.

2.3 Layered structures

The simplest layered structure where a film of refractive index n_0 coats a substrate of refractive index n_1 is shown in fig. 2.5. The medium above the film has refractive index n_2 and furthermore the three media are considered to be isotropic[4]. The procedure to be followed to obtain the effective amplitude reflection and transmission coefficients is due to Airy[5] and will be left as an exercise (2.2). The result can, both for p-waves and s-waves, be written as

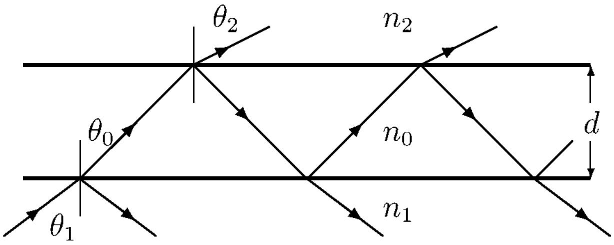

Fig. 2.5. Oblique reflection and transmission of a plane wave by a layered system with parallel-plane boundaries.

$$r = \frac{r_{10} + r_{02}e^{2i\varphi}}{1 + r_{10}r_{02}e^{2i\varphi}} \tag{2.7a}$$

$$t = \frac{t_{10}t_{02}e^{i\varphi}}{1 + r_{10}r_{02}e^{2i\varphi}} \tag{2.7b}$$

where r_{ij} and t_{ij} are the amplitude reflection and transmission coefficients respectively for the i to j interface, see eqs. (2.4a...2.4d). The phase angle φ arises from the optical path difference between the directly reflected light and the light that has

---

[3] The directions of p and s are chosen such as to form a right-handed Cartesian coordinate system with the direction of propagation.

[4] The more complex cases can be found in R.M.A. Assam and N.M. Bashara, *Ellipsometry and Polarized Light,* sec.4.7, North Holland, Amsterdam, 1977.

[5] G.B. Airy, *Phil. Mag.* 2 (1833) 20.

undergone one transmission into the film, one reflection and then again a transmission out of the film:

$$\varphi = \frac{2\pi n_0 d}{\lambda} \cos\theta_0. \tag{2.8}$$

Note that Snell's law still holds, i.e.

$$n_1 \sin\theta_1 = n_0 \sin\theta_0 = n_2 \sin\theta_2. \tag{2.9}$$

Since the films are usually thin, i.e. $d \ll \lambda$, the eqs. (2.7a) and (2.7b) are single-valued in d. For thick films this is no longer the case. The reason for this is in eq. (2.8): the phase angles φ and $\varphi + \pi$ result in identical reflection and transmission amplitude coefficients.

2.4 Thin films

The *ambient/film/substrate* system is often used as a model system in experimental situations. The layered structure of the previous section 2.3 is one of the crudest examples since the refractive index will in practice vary much less abrubtly then at the boundaries, see fig. 2.6.

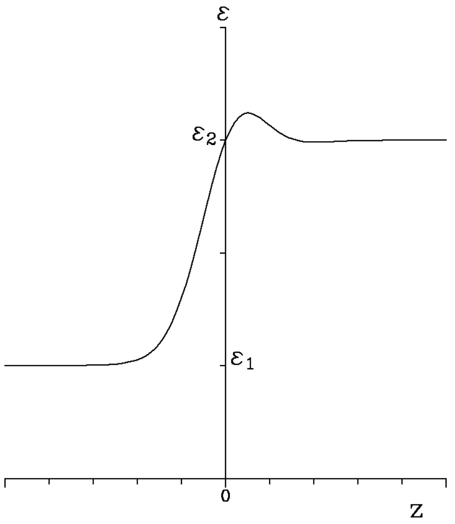

Fig. 2.6. Example of a dielectric permittivity profile with limiting values ϵ_1 and ϵ_2 far away from the interface.

Several methods have been developed in order to deal with more realistic systems. One method consists of extending the layered system of section 2.3 to a multilayer system upon which a limiting procedure is performed. In the limit of infinitesimally thin layers a continuous refraction index *profile* is obtained[6]. Another method treats the film as a *perturbation* to the ambient/substrate interface. It has been developed by Lekner for stratified media[7] and independently by Bedeaux and Vlieger for general surfaces[8].

---

[6] see R.M.A. Assam and N.M. Bashara, *Ellipsometry and Polarized Light*, sec.4.6, North Holland, Amsterdam, 1977.

For thin films the second method is the more appropriate because interface roughness can also be taken into account. Therefore this method is discussed below although for pedagogical purposes the system will at first be assumed to be stratified, i.e. the dielectric permittivity varies only in the z-direction perpendicular to the interface. At the end of this section surface roughness will be discussed briefly. Both ambient and substrate are supposed to be isotropic and all three media are nonmagnetic.

In the absence of a film, the dielectric permittivity profile is given by[9]

$$\epsilon_0(z) = \epsilon_1\theta(-z) + \epsilon_2\theta(z). \tag{2.10}$$

This profile gives rise to the Fresnel reflection and transmission amplitude coefficients discussed in section 2.2. An important aspect of the method is that not all of the details of the profile $\epsilon(z)$ need to be taken into account. For sufficiently thin films a very limited number of *moments* of the dielectric permittivity profile suffices. These moments are defined as integrals of the *excess* of the dielectric permittivity with respect to the *Fresnel* profile (2.10). Some of them are given by

$$\begin{aligned} j_{+,k+1} &= \left(\frac{2\pi}{\lambda}\right)^{k+1} \int z^k \{\epsilon(z) - \epsilon_0(z)\}\, dz \\ & \qquad\qquad\qquad\qquad\qquad\qquad k = 0, 1, 2, \ldots \\ j_{-,k+1} &= \left(\frac{2\pi}{\lambda}\right)^{k+1} \int z^k \left\{\frac{1}{\epsilon_0(z)} - \frac{1}{\epsilon(z)}\right\} dz, \end{aligned} \tag{2.11}$$

there are however more complicated moments. From the above definitions it is clear that the k-th moment is of k-th order in the *thickness* of the film[10] (with respect to the wavelength of the light). Another aspect is that the location of the origin of the coordinate system manifestly modifies the values of the moments. Obviously, the measurable quantities such as the reflectivity are independent of the location of the coordinate system. These are expressed in *invariant* combinations of the moments. One first order invariant moment is for instance constructed as $\mathcal{J}_1 \equiv j_{+,1} - \epsilon_1\epsilon_2 j_{-,1}$. For non-absorbing films the three lowest order *invariant moments* are: one of first order in film thickness

$$\mathcal{J}_1 = \frac{2\pi}{\lambda} \int \frac{\{\epsilon_1 - \epsilon(z)\}\{\epsilon(z) - \epsilon_2\}}{\epsilon(z)} dz \tag{2.12}$$

and two of second order in film thickness

$$\mathcal{J}_{21} = \left(\frac{2\pi}{\lambda}\right)^2 \int\int \frac{\epsilon_0(z - z')\{\epsilon(z) - \epsilon_0(z' - z)\}}{\epsilon_2 - \epsilon_1} dz dz'$$

---

[7] see J. Lekner, *Theory of Reflection*, chapters 3 and 8, Martinus Nijhoff Publ., Dordrecht 1987.

[8] see e.g. D. Bedeaux, G.J.M. Koper, E.A. v.d. Zeeuw, J. Vlieger, and M. Wind, *Physica* A 207 (1994) 285 and references therein.

[9] $\theta(z)$ is the *Heaviside* function: it is 1 for $z > 0$ and it is 0 for $z < 0$.

[10] The thickness of the film is size of the region in which the refractive index profile $\epsilon(z)$ differs from the Fresnel profile $\epsilon_0(z)$.

$$\times \left\{ \frac{1}{\epsilon(z')} - \frac{1}{\epsilon_0(z'-z)} \right\} \tag{2.13}$$

$$\mathcal{J}_{22} = -\left(\frac{2\pi}{\lambda}\right)^2 \int\int \frac{\{\epsilon(z)-\epsilon_0(z-z')\}\{\epsilon(z')-\epsilon_0(z'-z)\}}{\epsilon_2-\epsilon_1} dz dz'. \tag{2.14}$$

Absorbing films, however, have a complex dielectric permittivity and therefore also have two imaginary invariants of first order, $\mathrm{Im}(j_{-,1})$ and $\mathrm{Im}(j_{+,1})$. For simple profiles these invariants are easily calculated, see exercise 2.3.

For the reflectivity for s-waves for an absorbing film, the lowest order contribution comes from a first order imaginary invariant moment:

$$R_s = R_{s,0} - 4\,\mathrm{Im}(j_{-,1}) \frac{n_1 \cos\theta_1 (n_1 \cos\theta_1 - n_2 \cos\theta_2)}{(n_1 \cos\theta_1 + n_2 \cos\theta_2)^3} \tag{2.15}$$

where for non-absorbing films the lowest order contribution comes from a second order invariant moment

$$R_s = R_{s,0} - 2\epsilon_1 \mathcal{J}_{22} \frac{4 n_1 n_2 \cos\theta_1 \cos\theta_2}{(n_2 \cos\theta_1 + n_1 \cos\theta_2)^4}. \tag{2.16}$$

For the reflectivity for p-waves for an absorbing film the lowest order contribution is also from a first order imaginary invariant moment:

$$\begin{aligned} R_p &= R_{p,0} + \frac{4 n_1 \cos\theta_1 (n_2 \cos\theta_1 - n_1 \cos\theta_2)}{(n_2 \cos\theta_1 + n_1 \cos\theta_2)^3} \\ &\times \left\{ (\epsilon_1 \epsilon_2 \sin^2\theta_1\, \mathrm{Im}(j_{+,1}) - \cos^2\theta_2\, \mathrm{Im}(j_{-,1}) \right\} \end{aligned} \tag{2.17}$$

where for non-absorbing films the lowest order contribution is of second order in film thickness

$$\begin{aligned} R_p &= R_{p,0} + \frac{4 n_1 n_2 \cos\theta_1 \cos\theta_2}{(n_2 \cos\theta_1 + n_1 \cos\theta_2)^4} \\ &\times \left\{ -2(\mathcal{J}_{2,1} - \epsilon_1 \sin^2\theta_1 \mathcal{J}_{2,2})(\epsilon_2 \cos^2\theta_1 - \epsilon_1 \cos^2\theta_2) + \frac{\epsilon_1}{\epsilon_2} \sin^4\theta_1 \mathcal{J}_1^2 \right\} \end{aligned} \tag{2.18}$$

The values $R_{s,0} \equiv |r_{s,0}|^2$ and $R_{p,0} \equiv |r_{p,0}|^2$ are those found for the Fresnel profile $\epsilon_0(z)$. Contrary to the reflectivities, the ellipsometric ratio, cf. eq. (2.5), already has a contribution of first order both in the absorbing and in the non-absorbing case[11]

$$\frac{r_p}{r_s} = \frac{r_{p,0}}{r_{s,0}} - \frac{2\ \mathrm{i}\ n_1 \cos\theta_1 \sin^2\theta_1}{r_{s,0}(n_2 \cos\theta_1 + n_1 \cos\theta_2)^2} \mathcal{J}_1. \tag{2.19}$$

The case of reflection by a thin film between like media where $\epsilon_1 = \epsilon_2$, like soap films, requires special attention[12]. For the Fresnel profile the Brewster angle is defined by eq. (2.6). In ellipsometry it is common practice to define the Brewster angle as the angle for which the ellipsometric angle Δ (see eq. (2.5)) vanishes. The shift in the position of this Brewster angle due to the film is of second order in the film thickness. The contribution to the ellipsometric ratio at the Brewster angle is (for the Fresnel profile it vanishes)

---

[11] This formula is often attributed to Drude, but was, in essence, first obtained by L. Lorenz in 1860.

[12] see for instance J. Lekner, *Theory of Reflection*, chapter 3, Martinus Nijhoff Publ., Dordrecht 1987.

$$\left|\frac{r_p}{r_s}(\theta_B)\right| = \frac{\sqrt{\epsilon_2+\epsilon_1}}{2|\epsilon_2-\epsilon_1|}\mathcal{J}_1. \tag{2.20}$$

For non-absorbing films, as discussed above, the contributions to the reflectivities and the ellipsometric ratio is small. The notable exeption is the p-wave reflectivity and the ellipsometric ratio near the Brewster angle. Therefore most experiments are carried out near this Brewster angle as will be discussed in section 2.5.

The important result of the work of Bedeaux and Vlieger is that the functional form of the reflectivities (2.15, 2.16, 2.17, 2.18) and the ellipsometric ratio are preserved when interface roughness is introduced. The interpretation of the *invariant moments* however is completely different. For instance for a film consisting of a low density ϑ of small dielectric spheres (radius a, polarizability α) Haarmans et al. calculate[13]

$$\mathcal{J}_1 \simeq \frac{2\pi}{\lambda}\vartheta\alpha\left(1-\frac{\epsilon_1}{\epsilon_2}\right) \tag{2.21}$$

$$\mathcal{J}_{21} \simeq -\left(\frac{2\pi}{\lambda}\right)^2\vartheta\alpha a \tag{2.22}$$

$$\mathcal{J}_{22} \simeq -\frac{2}{\epsilon_2}\left(\frac{2\pi}{\lambda}\right)^2\vartheta\alpha a \tag{2.23}$$

where it is assumed that the dielectric permittivity of the spheres is close to the permittivities of both the medium and the ambient. More exact formulae can be obtained from the cited paper.

2.5 Experimental techniques

In this section three techniques that can be used to study the reflection from interfaces will be discussed.

2.5.1 Null ellipsometry

In its simplest form a null ellipsometer consists of two telescope arms (see fig. 2.7)[14]. One arm holds a light source such as a small laser, a polarizer, and a linear retarder. This arm directs the light to a reflecting surface, the sample. The angle of incidence can be chosen by means of a goniometer that rotates either the arm or the sample. The other arm, holding an analyzer and a photodetector, can be rotated around the sample in order to direct the reflected light from the sample into the photodetector.

To analyze this setup we assign angles θ_p, θ_r, and θ_a to the orientation with respect to the plane of incidence of the fast axes of the polarizer, the linear retarder, and the analyzer respectively. After the polarizer the light, which is assumed to be of unity

---

[13] M. Haarmans and D. Bedeaux, *Thin Solid Films* 224, 1994, 117, *Physica* A 207 (1994) 340.

[14] see R.M.A. Assam and N.M. Bashara, *Ellipsometry and Polarized Light*, chapter 3, North Holland, Amsterdam, 1977.

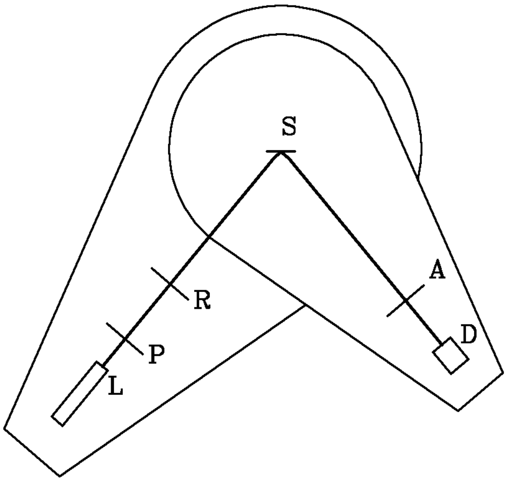

Fig. 2.7. Null ellipsometer with on one arm the laser (L), the polarizer (P), and the linear retarder (R). In the middle the surface under study (S), and on the other arm the analyzer (A) and the photodetector (D).

intensity, has Jones vector $(\cos\theta_p, \sin\theta_p)$. The transfer matrix of the linear retarder is written as

$$\begin{pmatrix} 1 & 0 \\ 0 & \rho_r \end{pmatrix} \tag{2.24}$$

where ρ_r is simply i for an ideal quarter wavelength retarder. Calling the amplitude reflection coefficients of the sample r_s and r_p, the electric field of the light impinging on the photomultiplier for unity incident intensity is given by

$$\begin{aligned} E_D &= \begin{pmatrix} \cos^2\theta_a & \cos\theta_a\sin\theta_a \\ \cos\theta_a\sin\theta_a & \sin^2\theta_a \end{pmatrix} \begin{pmatrix} r_p & 0 \\ 0 & r_s \end{pmatrix} \\ &\times \begin{pmatrix} \cos^2\theta_r + \rho_r\sin^2\theta_r & (1-\rho_r)\cos\theta_r\sin\theta_r \\ (1-\rho_r)\cos\theta_r\sin\theta_r & \sin^2\theta_r + \rho_r\cos^2\theta_r \end{pmatrix} \begin{pmatrix} \cos\theta_p \\ \sin\theta_p \end{pmatrix} \end{aligned} \tag{2.25}$$

The condition(s) for which the detector signal vanishes gives the ellipsometric ratio

$$\frac{r_p}{r_s} = -\tan\theta_a \frac{\tan\theta_r + \rho_r\tan(\theta_p - \theta_r)}{1 - \rho_r\tan\theta_r\tan(\theta_p - \theta_r)}. \tag{2.26}$$

An advantage of the technique is that this result does not depend on the intensity of the incident light. Of course the accuracy with which the nulling angles can be obtained does depend on light intensity. Null ellipsometry can be used in cases where the film (or the substrate) is absorbing. As discussed in the previous section, the contribution of dielectric films to the ellipsometric ratio is small except near the Brewster angle. But even then the ellipsometric ratio is smaller than 10^{-3} (it is 0 for the Fresnel profile). Small errors in the nulling angles introduce too large an error in the ellipsometric ratio to use this technique succesfully for these films[15].

2.5.2 Polarization modulation ellipsometry

There are two situations where nulling ellipsometry is not the technique of choice. The one situation is where the sensitivity of the technique is insufficient as discussed before and the other situation is where speed is needed in order to follow for example an adsorption process. In those situations polarization modulation ellipsometry is the better choice since it is fast, accurate and less sensitive than nulling ellipsometry to the alignment. The technique is used by Meunier[16] after the design of Jasperson and Schnatterly[17] and Beaglehole[18]. The optical arrangement is almost identical to the nulling ellipsometer, see fig. 2.7. It has no linear retarder and there are two additional elements, a polarization modulator operating at a high frequency of approximately 50 kHz between the polarizer and the sample and one operating at a low frequency (of approximately 10 Hz) between the sample and the analyzer. The polarizer is oriented at 45° with respect to the plane of incidence so that the electric field has equal s and p amplitudes. The first modulator introduces a time dependent phase shift $\delta = \delta_0 \sin \omega t$ between the s and p components. The phase amplitude δ_0 can be controlled by the amplitude of the voltage applied to the modulator. After reflection at the surface the light passes through the second modulator that is operated at a low frequency. This modulator is calibrated such that it introduces a phase shift of either 0 or π radians between the p and the s component at the low switching frequency. Then the light passes through the analyzer that is oriented at 45° with respect to the plane of incidence and impinges onto the photodetector. The action of both the second modulator and the analyzer is that of an analyzer switching between +45° and −45° with respect to the plane of incidence. Usually the photodetector is equipped with a pinhole to reduce the influence of stray light[19].

The analysis of this configuration starts by writing down the Jones vector of the electric field at the detector for unity incident intensity

$$E_D = \frac{1}{2\sqrt{2}} \begin{pmatrix} 1 & \pm 1 \\ \pm 1 & 1 \end{pmatrix} \begin{pmatrix} r_p & 0 \\ 0 & r_s \end{pmatrix} \begin{pmatrix} e^{i\delta} & 0 \\ 0 & 1 \end{pmatrix} \begin{pmatrix} 1 \\ 1 \end{pmatrix} \tag{2.27}$$

and after some algebra one finds that the intensity $E_D E_D^*$ at the detector is proportional to

$$I_D \sim |\rho|^2 \pm 2|\rho| \cos(\Delta + \delta) + 1 \tag{2.28}$$

---

[15] There is however the notable exception of C. Bouhet, *Ann Phys (Paris)* 15 (1931) 3, who used the technique for surfactant films!

[16] J. Meunier, *J Phys (Paris) Lett* 46 (1985) L-1005.

[17] S.N. Jasperson and S.E. Schnatterly, *Rev Sci Instr* 40 (1969) 761.

[18] D. Beaglehole, *Physica B* 100 (1980) 163.

[19] The size of this pinhole is not always unimportant as it determines the collection angle for scatter contributions from the interface, see for instance J. Meunier, *J Physique* 48 (1987) 1819 and E.M. Blokhuis and D. Bedeaux, *J Chem Phys* 95 (1990) 13.

where $|\rho|$ is the absolute value of the ellipsometric ratio and Δ its phase. As $\delta = \delta_0 \sin \omega t$ the detector signal will contain besides a constant (0) component also components at frequency ω, 2ω, etc. The first few components are given by

$$\begin{aligned} I_0 &\sim |\rho|^2 \pm 2|\rho| J_0(\delta_0) \cos \Delta + 1 \\ I_\omega &\sim \pm 4|\rho| J_1(\delta_0) \sin \omega t \sin \Delta \\ I_{2\omega} &\sim \pm 4|\rho| J_2(\delta_0) \cos 2\omega t \cos \Delta, \end{aligned} \tag{2.29}$$

where J_n is the Bessel function of order n. The procedure is now as follows: the low frequency switching of the signal makes it possible to find the phase amplitude δ_0 at which $J_0(\delta_0) = 0$: then I_0 remains constant while the modulator switches. The value of δ_0 at which this occurs is precisely known and therefore also the values of $J_1(\delta_0)$ and $J_2(\delta_0)$ are known constants. From the remaining signals I_0, I_ω, and $I_{2\omega}$ the ellipsometric ratio can be determined.

2.5.3 Ellipsometry data analysis

Both ellipsometry techniques provide the ellipsometric ratio. Without an underlying model this (complex) number is useless. In some instances one does have a model, such as the capillary wave model for fluid/fluid interfaces that will be discussed in the next chapter 3. More often there is no model at hand and one takes the default *thin film* model. The best situation is when both the ambient and the substrate are well characterized, i.e. the refractive indices are known and the uncoated interface is sufficiently *smooth* so that it does not act as a surface film itself. When these conditions are fulfilled, the ellipsometric ratio determines the (complex) first invariant moment $\mathcal{J}_1$ through eq. (2.19). Again, when no information is available on the dielectric permittivity profile one usually takes the simplest case of a homogeneous film of dielectric permittivity ϵ with a thickness d. For such a film the first invariant is

$$\mathcal{J}_1 = \frac{2\pi d}{\lambda} \frac{(\epsilon_1 - \epsilon)(\epsilon - \epsilon_2)}{\epsilon}. \tag{2.30}$$

The choice of the dielectric permittivity determines the thickness d that one will find: one finds an *ellipsometric thickness.* When a homogenous film of some material is adsorbed one may choose the dielectric permittivity of the bulk material. For discontinuous island films a method by Maxwell Garnett[20] is rather popular. Calling ϵ_0 the dielectric permittivity of the film material and φ the volume fraction taken by the material rather than by the ambient in the film the effective dielectric permittivity ϵ is found from

$$\frac{\epsilon - \epsilon_2}{\epsilon + 2\epsilon_2} = \varphi \frac{\epsilon_0 - \epsilon_2}{\epsilon_0 + 2\epsilon_2}, \tag{2.31}$$

a formula that can easily be derived from the Clausius-Mossotti or Lorentz-Lorenz relation (1.27). A better approach to discontinuous films is the sphere model discussed at the end of section 2.4.

---

[20] see R.M.A. Assam and N.M. Bashara, *Ellipsometry and Polarized Light*, section 4.8, North Holland, Amsterdam, 1977.

An important application of ellipsometry is spectroscopy where the wavelength of the light is varied. With this technique, in particular when infrared light is used, it is possible to identify the adsorbed molecules at the interface. Even the type of binding to the substrate can sometimes be determined.

2.5.4 Reflectometry around the Brewster angle

The main drawback of ellipsometry is that it is practically impossible to obtain more information on the interfacial region than the first invariant moment. Even the determination of the ellipsometric ratio at a number of different incidence angles does not really improve this situation because usually the first invariant will dominate. This is not the case for p-wave reflectivity of dielectric films, see eq. (2.18). When p-wave reflectivities are collected near the Brewster angle, where the Fresnel contribution $R_{p,0}$ is small, both second invariant moments and the first invariant moment (squared) can be determined[21].

The optical arrangement of a reflectometer is even simpler than the null ellipsometer, see fig. 2.7: there is no linear retarder[22]. The simplicity of the instrument allows for a variation of the incidence and detection angle. The technical difficulty is to keep the telescope arms in the plane of incidence of the reflecting interface.

Exercises

2.1 Argue that a random assembly of scatterers all lying in the same plane obey the law of reflection.

2.2 Derive eqs. (2.7a, 2.7b) for the reflection and transmission amplitudes of a bilayer.

2.3 Calculate the invariants $\mathcal{J}_1$, $\mathcal{J}_{21}$, and $\mathcal{J}_{22}$ for the homogenous film of dielectric permittivity ϵ and thickness d.

2.4 In a *poor man's ellipsometer*[23] one measures R_p/R_s rather than the ellipsometric ratio r_p/r_s and hence one determines $\mathcal{J}_1^2$ (see eq.(2.19)). Demonstrate that the sensitivity of the method can be greatly improved by pre-adsorbing a layer of given ellipsometric thickness $\mathcal{J}_{1,0}$.

---

[21] Note that the p-wave reflectivity is *linear* in $\mathcal{J}_1^2$, $\mathcal{J}_{21}$ and $\mathcal{J}_{22}$.

[22] see G.J.M. Koper and P. Schaaf, *Europhys Lett* 22 (1993) 543.

[23] see J.C. Dijt, M.A. Cohen Stuart, J.E. Hofman, and G.J. Fleer, *Colloids and Surfaces* 51 (1990) 141 - 158.

3 Reflection at fluid/fluid interfaces

3.1 The capillary wave model

Consider the interface between two (immiscible) fluids. Below the interface the density is ρ_1 and the dielectric permittivity is ϵ_1, and above the interface these are ρ_2 and ϵ_2 respecitively. A coordinate system is chosen such that the z-axis is perpendicular to the interface. The separation between the two fluids is a corrugated interface $\zeta(\boldsymbol{x})$, where $\boldsymbol{x}$ is a (2-dimensional) vector in the xy-plane. Across this interface all physical properties change abruptly from their one value to the other. The interface does have a surface tension and a bending elasticity that try to keep the interface flat. However, due to thermal agitation it fluctuates constantly around its mean value $\langle\zeta\rangle = 0$ such that the interface appears to have a finite thickness $\langle\zeta^2\rangle$. In the following section an expression for $\langle\zeta^2\rangle$ will be derived and in section 3.1.2 the reflectivity of such an interface will be calculated.

3.1.1 Statistical thermodynamics

The statistical mechanical treatment consists of replacing the time-averages of the fluctuating interface by the associated ensemble averages over all possible corrugated interfaces weighted by their free energies.

As a reference state the flat interface, $\zeta(\boldsymbol{x}) \equiv 0$ is chosen. The first contribution to the free energy of an arbitrary corrugated interface $\zeta(\boldsymbol{x})$ is the hydrostatic energy[1]

$$F_{\text{hydr}} = \frac{1}{2} \int\limits_S \Delta\rho \; g \; \zeta^2(\boldsymbol{x}) \; d^2x, \tag{3.1}$$

where $\Delta\rho \equiv \rho_1 - \rho_2$ and g is the gravitational accelaration. The second contribution comes from the increase in surface area with respect to the reference state

$$\Delta A = \int\limits_S \left\{ \sqrt{1 + |\boldsymbol{\nabla}\zeta(\boldsymbol{x})|^2} - 1 \right\} \; d^2x \simeq \frac{1}{2} \int\limits_S |\boldsymbol{\nabla}\zeta(\boldsymbol{x})|^2 \; d^2x, \tag{3.2}$$

where it is assumed that the gradients in the corrugations are small. The increase in free energy is therefore

$$F_{\text{surf}} = \gamma \Delta A = \frac{\gamma}{2} \int\limits_S |\boldsymbol{\nabla}\zeta(\boldsymbol{x})|^2 \; d^2x, \tag{3.3}$$

where γ is the surface tension. The third contribution comes from the bending of the interface with respect to the reference state. For small corrugation curvature $|\nabla^2\zeta|$ it is given by[2]

$$F_{\text{curv}} \simeq \frac{\kappa}{2} \int\limits_S |\nabla^2\zeta(\boldsymbol{x})|^2 \; d^2x, \tag{3.4}$$

---

[1] The surface integrals extend over a macroscopic surface S

[2] see W. Helfrich, *Z Naturforsch C* 28 (1973) 693.

where κ is the bending elasticity modulus. In principle it is possible to include more contributions to the free energy of a corrugated interface. It is believed that the three mentioned contributions are sufficient to model real liquid/liquid interfaces.

At this stage it is useful to introduce 2-dimensional Fourier-transformed quantities $\hat{\zeta}(\boldsymbol{q})$ such that

$$\zeta(\boldsymbol{x}) = \int \hat{\zeta}(\boldsymbol{q})\ \exp(\mathrm{i}\ \boldsymbol{q}\cdot\boldsymbol{x})\ d^2q. \tag{3.5}$$

Each value of $\boldsymbol{q}$ represents a capilary *wave* or *mode*, hence the name of the model. The total free energy of a corrugated interface $\zeta(\boldsymbol{x})$ is, with eq.(3.5), written as

$$F = 2\pi^2 \int \left\{\Delta\rho\ g + \gamma q^2 + \kappa q^4\right\} |\hat{\zeta}(\boldsymbol{q})|^2\ d^2q. \tag{3.6}$$

In order to find the mean squared thickness the thickness of all corrugated interfaces, weighted with their appropriate Boltzmann factors, have to be averaged. This is identical to averaging the thicknesses of all modes with the appropriate Boltzmann factors. Since each mode represents one degree of freedom the equipartition theorem states that the free energy associated with each such mode equals $k_BT/2$:

$$\langle|\hat{\zeta}(\boldsymbol{q})|^2\rangle = \frac{k_BT}{(2\pi)^2(\Delta\rho\ g + \gamma q^2 + \kappa q^4)}. \tag{3.7}$$

The mean squared thickness of the interface is now calculated as

$$\begin{aligned} \langle\zeta^2\rangle &= \int \langle|\hat{\zeta}(\boldsymbol{q})|^2\rangle\ d^2q \\ &= \frac{k_BT}{2\pi} \int_0^{q_{\text{max}}} \frac{q}{\Delta\rho\ g + \gamma q^2 + \kappa q^4}\ dq \\ &= \frac{k_BT}{4\pi\gamma} \log\left\{\frac{1 + q_{\text{max}}^2 L_c^2}{1 + q_{\text{max}}^2 L_b^2}\right\} \end{aligned} \tag{3.8}$$

with the capillary wavelength $L_c^2 = \gamma/\Delta\rho\ g$ and the bending length $L_b^2 = \kappa/\gamma$. The maximum wavenumber q_{max} is determined by experimental conditions. In particular it cannot be larger than the inverse molecular spacing. When both the capillary wavelength L_c and the bending length L_b are not too small the resulting mean squared thickness is independent of q_{max}. The first length to become too small is the bending length L_b. Then the resulting mean squared thickness depends on the maximum wavenumber q_{max}[3].

For too large corrugations and corrugation gradients the linear approximations that have been made to derive the free energy of a corrugated interface are no longer correct. For sufficiently small nonlinearities a mode-coupling theory has been developed by J. Meunier[4].

---

[3] see J. Meunier, *J. Phys. Lett. (France)* 46 (1985) 1005-1014.

[4] see J. Meunier, *J. Phys. (France)* 48 (1987) 1819-1831.

3.1.2 Reflectivity

For quite some time it was believed that the finite thickness $\langle\zeta^2\rangle$ of the corrugated interface was the important contribution to its reflectivity. It is still instructive to repeat the argument as the exact theory is too complicated to render in these notes[5]. As a first step the averaged interfacial composition is calculated. For simplicity it is assumed that the two fluids are two phases of one and the same type, such as a liquid and a gas phase:

$$\rho(z) = \rho_1 + (\rho_2 - \rho_1)\langle\theta(z - \zeta(\boldsymbol{x}))\rangle \tag{3.9}$$

The average of the Heaviside function is calculated using the identity

$$\theta(u) = \int\limits_{-\infty}^{u} \delta(u')\, du' \tag{3.10}$$

and by subsequently introducing the Fourier-integral representation of the delta-function

$$\delta(u) = \frac{1}{2\pi}\int e^{\mathrm{i}\alpha u}\, d\alpha. \tag{3.11}$$

Substitution of these identities in eq.(3.9) yields

$$\rho(z) = \rho_1 + (\rho_2 - \rho_1)\int\limits_{-\infty}^{z} \frac{1}{2\pi}\int d\alpha\; e^{\mathrm{i}\alpha u}\langle\exp\left(-\mathrm{i}\alpha\zeta(\boldsymbol{x})\right)\rangle\, du. \tag{3.12}$$

The average of the exponential is calculated with the following “trick”

$$\begin{aligned}\langle\exp\left(-\mathrm{i}\alpha\zeta(\boldsymbol{x})\right)\rangle &= \exp\log\left\{1 - \mathrm{i}\alpha\langle\zeta\rangle - \tfrac{1}{2}\alpha^2\langle\zeta^2\rangle + \ldots\right\}\\ &= \exp\left\{-\mathrm{i}\alpha\langle\zeta\rangle - \tfrac{1}{2}\alpha^2(\langle\zeta^2\rangle - \langle\zeta\rangle^2) + \ldots\right\}.\end{aligned} \tag{3.13}$$

Since $\langle\zeta\rangle = 0$ the leading contribution is due to the thickness $\langle\zeta^2\rangle$:

$$\langle\exp\left(-\mathrm{i}\alpha\zeta(\boldsymbol{x})\right)\rangle \simeq \exp\left\{-\frac{\alpha^2}{2}\langle\zeta^2\rangle\right\} \tag{3.14}$$

Finally one obtains from eq.(3.9) the result

$$\rho(z) = \frac{\rho_2 + \rho_2}{2} + \frac{\rho_1 - \rho_2}{2}\,\mathrm{erf}\left(\frac{z}{\sqrt{2\langle\zeta^2\rangle}}\right) \tag{3.15}$$

with the error function defined as

$$\mathrm{erf}(z) = \frac{1}{\sqrt{\pi}}\int\limits_{0}^{z} e^{-t^2}\, dt. \tag{3.16}$$

Through the Lorentz-Lorenz equation (1.27) the averaged dielectric permittivity profile $\epsilon(z)$ is related to the averaged density profile (3.15). An almost identical result is obtained by using the (simpler) density-weighted average of the dielectric permittivity

---

[5] see F.P. Buff, R.A. Lovett, and F.H. Stillinger Jr. *Phys. Rev. Lett.* 15 (1963) 621.

$$\begin{aligned}\epsilon(z) &= \frac{\epsilon_1\{\rho_1-\rho(z)\}+\epsilon_2\{\rho(z)-\rho_2\}}{\rho_1-\rho_2} \\ &= \frac{\epsilon_1+\epsilon_2}{2}+\frac{\epsilon_1-\epsilon_2}{2}\,\mathrm{erf}\left(\frac{z}{\sqrt{2\langle\zeta^2\rangle}}\right) \qquad (3.17)\end{aligned}$$

At the Brewster angle the ellipsometric ratio is determined by the first invariant moment (2.12) which for this situation is given by[6]:

$$\begin{aligned}\mathcal{J}_1 &= \frac{2\pi}{\lambda}\frac{\epsilon_1-\epsilon_2}{\epsilon_1+\epsilon_2}\int\frac{1-\mathrm{erf}^2\left(\frac{z}{\sqrt{2\langle\zeta^2\rangle}}\right)}{1+\frac{\epsilon_1-\epsilon_2}{\epsilon_1+\epsilon_2}\,\mathrm{erf}\left(\frac{z}{\sqrt{2\langle\zeta^2\rangle}}\right)}\,dz \\ &= \frac{2\pi}{\lambda}\frac{\epsilon_1-\epsilon_2}{\epsilon_1+\epsilon_2}\sqrt{2\langle\zeta^2\rangle}\int\frac{1-\mathrm{erf}^2(u)}{1+\frac{\epsilon_1-\epsilon_2}{\epsilon_1+\epsilon_2}\,\mathrm{erf}(u)}\,du \qquad (3.18)\end{aligned}$$

For the thickness $\langle\zeta^2\rangle$ the expression (3.8) can be used. This formula is *not correct* as it does not have the temperature dependence and the dependence on surface tension as have been found by experiment. The above given derivation is wrong in neglecting the effect of the slopes of the corrugated surface. These introduce phase differences between the p and the s waves that can only be properly accounted for by applying Maxwell's equations to the interfacial regime. The result of such an analysis is[7]

$$\mathcal{J}_1 = -\frac{3\pi}{\lambda}\frac{(\epsilon_1-\epsilon_2)^2}{\epsilon_1+\epsilon_2}\int q\langle|\hat{\zeta}(\boldsymbol{q})|^2\rangle\,d^2q. \qquad (3.19)$$

The integral over $\boldsymbol{q}$ is easily evaluated in the limit of the capillary length $L_c \to \infty$[8]:

$$\int q\langle|\hat{\zeta}(\boldsymbol{q})|^2\rangle\,d^2q = \frac{k_BT}{2\pi\sqrt{\gamma\kappa}}\arctan(q_{\mathrm{max}}L_b) \qquad (3.20)$$

For not too large a bending length L_b the result is independent of q_{max}:

$$\mathcal{J}_1 \simeq -\frac{3\pi}{4\lambda}\frac{(\epsilon_1-\epsilon_2)^2}{\epsilon_1+\epsilon_2}\frac{k_BT}{\sqrt{\gamma\kappa}}. \qquad (3.21)$$

The thickness $\langle\zeta^2\rangle$ does play a role in the reflectivity of corrugated interfaces: the two second invariant moments (see eqs.(2.13,2.14)) are proportional to this thickness.

---

[6] see D. Beaglehole, *Physica B* 100 (1980) 163.

[7] see B.J.A. Zielinska, D. Bedeaux, and J. Vlieger, *Physica A* 107 (1981) 91.

[8] see E.M. Blokhuis and D. Bedeaux, *Physica A* 164 (1990) 515.

3.2 Application

The direct application of the capillary wave model is hampered by the fact that realistic interfaces are not ideal, i.e. the dielectric permittivity does not step from one into the other value across the interface. From their general theory for rough surfaces Bedeaux and Vlieger find that if several surface inhomogeneities are present, the nett invariant moments are the sum of the separate contributions. So the above derived roughness term is at least to be added to a term due to the *intrinsic* density profile.

For the interface between two fluid phases the classical density profile of the Van der Waals and Cahn-Hilliard theories can be used[9]

$$\rho(z) = \frac{\rho_1 + \rho_2}{2} + \frac{\rho_1 - \rho_2}{2} \tanh\left(\frac{2z}{\xi}\right). \tag{3.22}$$

This density profile is to be substituted in the expression (2.12) for the first invariant moment using the Lorentz-Lorenz relation (1.27). Far from the critical point the correlation length ξ is small and the interface is almost like a step function. But as the critical point is approached, the interface thickens and becomes diffuse, until, at the critical point, it disappears completely and the two phases become identical. More complicated interfaces require a more detailed model for the dielectric permittivity profile.

The apparent dependence of the ellipsometric ratio at the Brewster angle on bending elasticity modulus and surface tension as expressed by the first invariant moment (3.21) has been utilized by Meunier to determine the bending elasticity of surfactant monolayers at the planar oil/water interface[10]. By varying the salt concentration of the water phase samples with different surface tension and the same bending elasticity are prepared. The surface tension is determined independently. The obtained ellipsometric ratios plotted versus $1/\sqrt{\gamma}$ gives a straight line from which the bending elasticity modulus can be determined. The success of the experiment not only demonstrates the correctness of the assumption of constant bending elasticity but also demonstrates the applicability of the capillary wave model.

Exercises

3.1 Derive eq.(3.1).

3.2 Show that the capillary wave model in one dimension does not need the introduction of a bending elasticity modulus to obtain a mean squared thickness that is independent of a maximum wavenumber.

---

[9] see J. Van der Waals, *Z. Phys. Chem.* 13 (1894) 657 and J.W. Cahn and J.E. Hilliard, *J. Chem. Phys.* 28 (1958) 3219.

[10] see for instance B.P. Binks, H. Kellay, and J. Meunier, *Thin Solid Films* 210/211 (1992) 118-120.

4 Light scattering by single particles

The scattering of light is described by van de Hulst[1] and by Kerker[2]. In these notes some important aspects of light scattering by single particles will be highlighted.

4.1 Rayleigh theory of scattering by small dielectric spheres

Consider a small dielectric sphere in the origin of a Cartesian coordinate system. The sphere has radius a and dielectric permittivity ϵ_2 whereas the ambient medium has dielectric permittivity ϵ_1. The dipole polarizability of such a sphere is[3], see exercise 4.1.

$$\alpha = 4\pi a^3 \epsilon_1 \frac{\epsilon_2 - \epsilon_1}{\epsilon_2 + 2\epsilon_1}. \tag{4.1}$$

An incident electromagnetic field with electric field vector

$$\boldsymbol{E}_i = \boldsymbol{E}_{i,0} e^{-\mathrm{i}\omega t} \tag{4.2}$$

induces in the sphere an oscillating dipole moment

$$\boldsymbol{p} = \alpha \boldsymbol{E}_{i,0} e^{-\mathrm{i}\omega t}. \tag{4.3}$$

Thus, the dielectric sphere acts as an electric dipole which radiates *scattered* waves in all directions. The wavenumber $k = 2\pi n_1/\lambda$ where the refractive index $n_1 = \sqrt{\epsilon_1}$ and λ is the wavelength of the light in vacuum. In a far point $\boldsymbol{r}$, $kr \gg 1$, the scattered electric field is given by[4]

$$\boldsymbol{E} = k^2 (\hat{\boldsymbol{r}} \times \boldsymbol{p}) \times \hat{\boldsymbol{r}} \frac{e^{\mathrm{i}kr}}{4\pi\epsilon_1 r} \tag{4.4}$$

where $\hat{\boldsymbol{r}}$ is a unit vector in the direction $\boldsymbol{r}$, i.e. $\hat{\boldsymbol{r}} = \boldsymbol{r}/r$. The direction of propagation is along $\hat{\boldsymbol{r}}$ and the magnetic field vector is perpendicular to both the electric field and the direction of propagation.

In what follows we shall assume that the incident light propagates along the z-axis of the coordinate system. The observer is located in the xz-plane, which is then called the *scattering plane*, at a *scattering angle* θ with respect to the z-axis, see fig. 4.1. For p-polarized incidence light, i.e. light that is polarized in the scattering plane, the scattered intensity is

$$I_p = I_i \frac{16\pi^4 a^6}{\lambda^4 r^2} \left(\frac{\epsilon_2 - \epsilon_1}{\epsilon_2 + 2\epsilon_1} \right)^2 \cos^2\theta \tag{4.5a}$$

where $I_i = \epsilon_1 \boldsymbol{E_i} \cdot \boldsymbol{E_i}^*$ is the incident light intensity. For s-polarized light, i.e. light that is polarized perpendicular to the scattering plane, the scattered intensity is

$$I_s = I_i \frac{16\pi^4 a^6}{\lambda^4 r^2} \left(\frac{\epsilon_2 - \epsilon_1}{\epsilon_2 + 2\epsilon_1} \right)^2. \tag{4.5b}$$

---

[1] H.C. van de Hulst, *Light Scattering by Small Particles*, Dover, NY 1957.

[2] M. Kerker, *The Scattering of Light and Other Electromagnetic Radiation*, Academic Press, NY 1969.

[3] see: J.D. Jackson, *Classical Electrodynamics*, J. Wiley & Sons, New York 1975, sec. 4.4.

[4] see: J.D. Jackson, *Classical Electrodynamics*, J. Wiley & Sons, New York 1975, sec. 9.2.

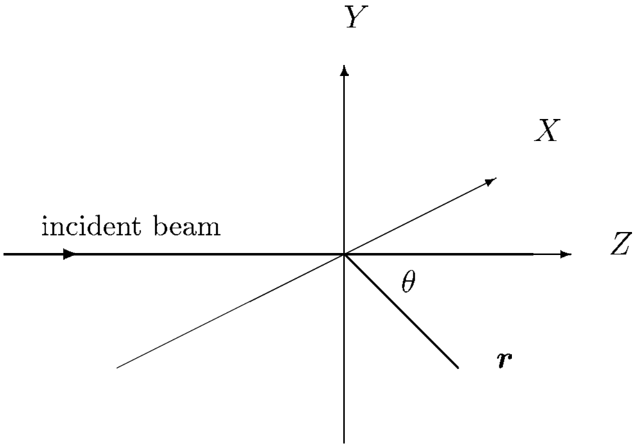

Fig. 4.1. Scattering geometry: the observer is at $\boldsymbol{r}$ in the xz-plane (the scattering plane) and θ is the scattering angle.

Unpolarized incident light can be resolved into two incoherent linear polarized components which are parallel and perpendicular to the scattering plane. In this case

$$I_u = \frac{I_p + I_s}{2} = I_i \frac{16\pi^4 a^6}{\lambda^4 r^2} \left(\frac{\epsilon_2 - \epsilon_1}{\epsilon_2 + 2\epsilon_1} \right)^2 (1 + \cos^2\theta). \tag{4.6}$$

A random distribution of small identical dielectric spheres scatters light incoherently and the total scattered intensity is the sum of the contributions of the individual spheres: the scattered intensity is proportional to the number of scatterers.

There are, in a historical perspective, two important consequences of the above given formulae: (1) the scattered intensity varies with $1/\lambda^4$ which accounts for the blue color of the sky and (2) for scattering angle $\pi/2$ the scattered light is *polarized* which accounts for the (partial) polarized sky light.

In the case of absorbing spheres the dielectric permittivity is a complex number and the computation of the intensities changes likewise.

4.2 Mie theory of scattering by spheres

The general theory of light scattering by spheres is given by Mie in 1908. The solution can be written in terms of two amplitude functions, one for p-polarized light

$$S_p(\theta) = \sum_{l=1}^{\infty} \frac{2l+1}{l(l+1)} \left\{ a_l \frac{dP_l^1(\cos\theta)}{d\theta} + b_l \frac{P_l^1(\cos\theta)}{\sin\theta} \right\} \tag{4.7a}$$

and one for s-polarized light

$$S_s(\theta) = \sum_{l=1}^{\infty} \frac{2l+1}{l(l+1)} \left\{ a_l \frac{P_l^1(\cos\theta)}{\sin\theta} + b_l \frac{dP_l^1(\cos\theta)}{d\theta} \right\}, \tag{4.7b}$$

where $P_l^m(z)$ are the associated Legendre functions of the first kind of degree l and of order m[5]. The coefficients a_l and b_l can be conveniently expressed in terms of angles α_l and β_l such that

$$a_l = \frac{\tan\alpha_l}{\tan\alpha_l - \mathrm{i}} \qquad \text{and} \qquad b_l = \frac{\tan\beta_l}{\tan\beta_l - \mathrm{i}}. \tag{4.8}$$

These angles, in turn, can be calculated by

$$\tan\alpha_l = -\frac{n_1\psi_l'(y)\psi_l(x) - n_2\psi_l(y)\psi_l'(x)}{n_1\psi_l'(y)\chi_l(x) - n_2\psi_l(y)\chi_l'(x)} \tag{4.9a}$$

and

$$\tan\beta_l = -\frac{n_2\psi_l'(y)\psi_l(x) - n_1\psi_l(y)\psi_l'(x)}{n_2\psi_l'(y)\chi_l(x) - n_1\psi_l(y)\chi_l'(x)} \tag{4.9b}$$

with $x = 2\pi n_1 a/\lambda$ and $y = 2\pi n_2 a/\lambda$. The Ricatti-Bessel functions ψ_l and χ_l are related to the spherical Bessel functions of the first kind j_l and of the second kind, y_l by

$$\psi_l(z) = z j_l(z) \qquad \text{and} \qquad \chi_l(z) = z y_l(z). \tag{4.10}$$

Great care has to be taken to evaluate the coefficients a_l and b_l numerically. It is for this reason that the coefficients are expressed in terms of the Ricatti-Bessel functions and not in the Hankel functions. Provided that one strictly follows the guidelines to evaluate these functions, as for instance put forward by Abramowitz and Stegun, the coefficients can be determined to any desired accuracy, see the appendix. The main reason to express the coefficients a_l and b_l in terms of the angles α_l and β_l, cf. eq.(4.8), is to reduce the amount of complex number manipulations.

For sufficiently large distances from the center of the sphere, i.e. $kr \gg 1$, the electric field of the scattered light for p-polarized incident light is also p-polarized with amplitude

$$E_p = E_i \frac{\mathrm{i}e^{-\mathrm{i}kr}}{kr} S_p(\theta) \tag{4.11a}$$

and the electric field of the scattered light for s-polarized incident light is s-polarized with amplitude

$$E_s = -E_i \frac{\mathrm{i}e^{-\mathrm{i}kr}}{kr} S_s(\theta). \tag{4.11b}$$

In fig. 4.2 some examples of scattering curves are given. The smallest latex sphere size (1 nm) is in the Rayleigh regime (the wavelength of the incidence light is chosen to be the HeNe line of 632.8nm) and this illustrates nicely the $\cos^2\theta$ behaviour characteristic of p-wave scattering. The scattering for larger particle sizes tends to concentrate in the forward direction.

---

[5] M. Abramowitz and I.A. Stegun, *Handbook of Mathematical Functions*, Dover, NY 1964.

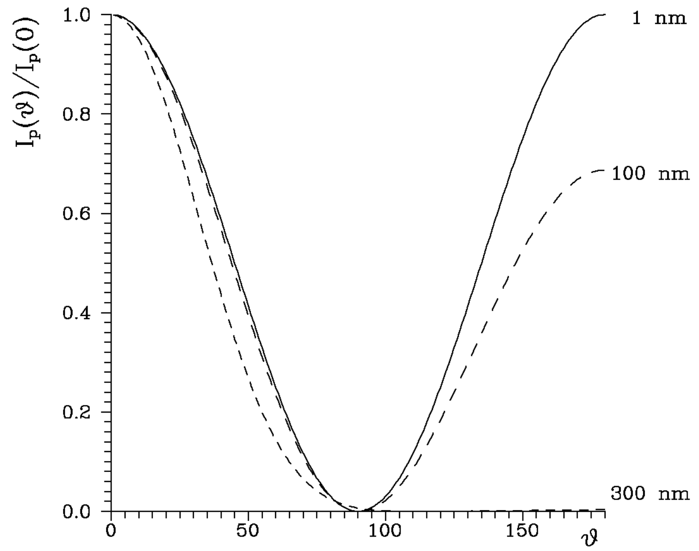

Fig. 4.2. Scattering intensities as a function of scattering angle for p-polarized incidence light of wavelength 632.8 nm. The particles are polystyrene latex spheres (n_l=1.6) dispersed in water (n_w=1.33).

4.3 Rayleigh-Gans-Debije scattering

Apart from the mentioned scattering functions for spheres there are also functions available of particles for other shapes such as stratified spheres and small ellipsoids and spheroids. These functions can be found in the monograph by Kerker. In this subsection we shall, rather then concentrate on a particular shape, discuss an approximate theory for particles of arbitrary shape and size. The quantum mechanical analog of this theory is known as the Born approximation.

The scattering function is calculated as follows: the particle, of arbitrary size and shape, is subdivided in infinitesimally small volume elements. Each such volume element is treated as a Rayleigh scatterer excited by the incident field which is supposed to be unperturbed by the prescence of the rest of the particle. For incident radiation polarized perpendicular to the scattering plane, the amplitude function for each volume element dV is given by

$$dS_s(\theta) = \mathrm{i}\frac{3k^3}{4\pi}\frac{\epsilon_2 - \epsilon_1}{\epsilon_2 + 2\epsilon_1}e^{\mathrm{i}\delta}dV, \tag{4.12}$$

where exp(iδ) relates the phase of each elemental wavelet at the position of the observer to a common reference plane perpendicular to the incidence beam. At the observation point, far removed from the particle, the resultant amplitude function which arises from interference of each of the contributions is obtained by vector summation

$$S_s(\theta) = \mathrm{i}\frac{3k^3}{4\pi}\frac{\epsilon_2 - \epsilon_1}{\epsilon_2 + 2\epsilon_1}\int e^{\mathrm{i}\delta} dV. \tag{4.13}$$

The fundamental approximation in this approach is that each volume element experiences the same incident field. For this reason neither the particle size nor the relative refractive index can become too large. For a relative refractive index $n \equiv \sqrt{\epsilon_2/\epsilon_1}$ sufficiently close to unity eq. (4.13) simplifies to

$$S_s(\theta) = \frac{\mathrm{i}k^3}{2\pi}(n-1)\int e^{\mathrm{i}\delta} dV. \tag{4.14}$$

For real refractive index one then has for s-polarized light

$$I_s(\theta) = \frac{k^4 V^2}{4\pi^2 r^2}(n-1)^2 P(\theta), \tag{4.15a}$$

and for p-polarized light

$$I_p(\theta) = \frac{k^4 V^2}{4\pi^2 r^2}(n-1)^2 P(\theta)\cos^2(\theta). \tag{4.15b}$$

The quantity $P(\theta)$ is known as the *form factor* and is given by

$$P(\theta) = \frac{1}{V^2}\left|\int e^{\mathrm{i}\delta} dV\right|^2. \tag{4.16}$$

The form factor has been evaluated for a variety of configurations. Rayleigh himself gave the result for a homogenous sphere with radius a

$$P(\theta) = \frac{3(\sin u - u\cos u)^2}{u^3} = \frac{9\pi}{2u^3}J^2_{3/2}(u) \tag{4.17}$$

where $u = 2ka\sin(\theta/2)$ and $J_{3/2}$ is the three-halves order Bessel function.

Debije formulated in 1915 the theory for an aggregate of discrete elements rather than for a continuum[6]. If each of the scattering elements is identical and the aggregate assumes all random orientations, then the following average form factor can be calculated

$$P(\theta) = \frac{1}{N^2}\sum_{i=1}^{N}\sum_{j=1}^{N}\frac{\sin qr_{ij}}{qr_{ij}} \tag{4.18}$$

where r_{ij} is the distance between centers of the elements and $q = 2k\sin(\theta/2)$. This expression has been evaluated for a number of configurations which are encountered in macromolecular chemistry. One of the most important applications being the randomly coiled high polymer chain for which Debije derived in 1947

$$P(\theta) = \frac{2(e^{-w} + w - 1)}{w^2} \tag{4.19}$$

where $w = q^2 R_g^2$ and R_g the radius of gyration of the polymer chain.

---

[6] see M. Kerker, *The Scattering of Light and Other Electromagnetic Radiation*, Academic Press, NY 1969, sec. 8.1.

4.4 Coupled-dipole method

In the Rayleigh-Gans-Debije approach to the scattering of particles of arbitrary shape and size the main assumption was that the local field for each volume element was the incident field. This is no longer the case in the *coupled-dipole method* for calculating the light scattering by nonspherical particles[7]. The method consists of dividing the object into an array of N subunits located on a simple cubic lattice. The subunits are asumed to be sufficiently small to give rise to only electric dipole radiation. Each subunit is characterized by a (symmetric) polarizability tensor α_j, such that the instantaneous dipole moment $\boldsymbol{p}_j$ can be expressed as

$$\boldsymbol{p}_j = \alpha_j \left(\boldsymbol{E}_j - \sum_{k \neq j} A_{jk} \boldsymbol{p}_k \right) \tag{4.20}$$

where $\boldsymbol{E}_j$ is the electric field at the site j due to the incident light. The second contribution to the electric field $-\sum_{k \neq j} A_{jk} \boldsymbol{p}_k$ is due to the dipoles at positions k. Defining the matrix elements

$$A_{jj} = \alpha_j^{-1} \tag{4.21}$$

one obtains the inhomogenous set of linear complex vector equations

$$\sum_{k=1}^{N} A_{jk} \boldsymbol{p}_k = \boldsymbol{E}_j. \tag{4.22}$$

The solution of this set of equations is a numerical problem and depending on the computational power at hand more or less success can be obtained.

The important issue left to discuss is the actual number to put in for the dipole polarizabilities α_j. The simplest approach is to use a Clausius-Mossotti or Lorentz-Lorenz relation (1.27) to calculate the polarizability. For spheres this does not always lead to satisfactory results compared to the exact Mie theory and one therefore often uses the electric dipole term of the Mie theory (4.8), i.e.

$$\alpha = \mathrm{i} \frac{6\pi}{k^3} a_1, \tag{4.23}$$

to obtain a better match. For nonspherical particles there is no way to assess the quality of the results apart from studying the convergence for increasing number N of subunits.

An important problem of the method is the spurious enhancement of the scattering induced by the cubic lattice. Techniques have been proposed to damp out these effects by adapting the polarizabilities α_j but, again, there is no way to assess the quality of the results for nonspherical particles.

---

[7] see C.E. Dungey and C.F. Bohren, *J Opt Soc Am A* 8 (1991) 81 and references therein.

Appendix: procedures to compute the scattering functions

Below a set of Turbo-Pascal (Borland, Scott's Valley, Ca.) procedures to calculate the Mie scattering functions for real refractive indices.

- Definition of types, constants, and global variables.

```
const
 l_max  =  10;     { largest order of multipole }
 lm_max =  65;     { l_max*(l_max+3)/2 }
 m_max  =  20;     { 2*l_max }
type
 real     = extended;
 l_array  = array [0..l_max] of real;
 lm_array = array [0..lm_max] of real;
var
 a_r,a_i,b_r,b_i         : l_array;
 Q                       : real;
 pie,tau                 : l_array;
 S1_r,S1_i               : real;
 S2_r,S2_i               : real;
 I1,I2                   : real;
```

- Procedures to compute the Ricatti-Bessel functions

```
procedure psi_calc(z : real; var psi,d_psi : l_array);
 const
  j_max = 100;
 var
  j          : array [0..j_max] of real;
  j0,p       : real;
  l          : integer;
 begin
  {
    Miller's algorithm utilizing recurrence relation backwards,
    see Abramowitz and Stegun, section 10.5
  }
  j[j_max]:=0;
  j[j_max-1]:=1;
  for l:=j_max-2 downto 0 do
   j[l]:=(2*l+3)*j[l+1]/z - j[l+2];
  j0:=sin(z)/z;
  p:=j0/j[0];
  psi[0]:=j0*z;
  for l:=1 to l_max do
   begin
    j[l]:=j[l]*p;
    psi[l]:=z*j[l];
    d_psi[l]:=-l*j[l]+psi[l-1];
   end;
 end;

procedure chi_calc(z : real; var chi,d_chi:l_array);
 var
  l          : integer;
  c,s        : real;
 begin
  {
    Simple forward recurrence relation algorithm,
    see Abramowitz and Stegun, section 10.5
  }
  c:=cos(z);
  s:=sin(z);
  chi[0]:=c;
  chi[1]:=c/z+s;
  d_chi[1]:=c*(1-1/sqr(z))-s/z;
  for l:=2 to l_max do
   begin
    chi[l]:=(2*l-1)*chi[l-1]/z-chi[l-2];
    d_chi[l]:=-l*chi[l]/z+chi[l-1];
   end;
 end;
```

- Procedure to compute the functions $\pi_l(\cos\theta) = P_l^1(\cos\theta)/\sin\theta$ and $\tau_l(\cos\theta) = \partial_\theta P_l^1(\cos\theta)$

```
procedure pie_tau_calc(z : real);
 var
  l          : integer;
  d_pie      : l_array;
  h          : real;
 begin
  {
    Simple forward recurrence relation algorithm,
    based on recursion relation for associated
    Legendre functions with m=1.
    See Van de Hulst, sec. 9.31, Kerker sec. 3.7.
    Note: pi is predefined by Turbo Pascal
  }
  h:=1-z*z;
  pie[1]:=1;     d_pie[1]:=0;
  pie[2]:=3*z;   d_pie[2]:=3;
  tau[1]:=z;
  tau[2]:=6*z*z-3;
  for l:=3 to l_max do
   begin
    pie[l]:=( (2*l-1)*z*pie[l-1] - l*pie[l-2] )/(l-1);
    d_pie[l]:=(2*l-1)*pie[l-1]+d_pie[l-2];
    tau[l]:=z*pie[l]-h*d_pie[l];
   end;
 end;
```

- Procedure to compute the coefficients a_l and b_l.

```
procedure ab_calc(q1,q3: real);
 var
  psi1,d_psi1,chi1,d_chi1 : l_array;
  psi3,d_psi3             : l_array;
  tan_a,tan_b             : real;
  l                       : integer;
  h                       : real;
 begin
  {
    Calculation of the coefficients a_l,b_l
    see Van de Hulst, p. 135
  }
  psi_calc(q1,psi1,d_psi1);
  psi_calc(q3,psi3,d_psi3);
  chi_calc(q1,chi1,d_chi1);
  Q:=0;
  for l:=1 to l_max do
   begin
    tan_a:=-(q1*d_psi3[l]*psi1[l]-q3*psi3[l]*d_psi1[l]);
    tan_a:=tan_a/(q1*d_psi3[l]*chi1[l]-q3*psi3[l]*d_chi1[l]);
    tan_b:=-(q3*d_psi3[l]*psi1[l]-q1*psi3[l]*d_psi1[l]);
    tan_b:=tan_b/(q3*d_psi3[l]*chi1[l]-q1*psi3[l]*d_chi1[l]);
    h:=tan_a*tan_a;
    a_r[l]:=h/(1+h);
    a_i[l]:=tan_a/(1+h);
    h:=tan_b*tan_b;
    b_r[l]:=h/(1+h);
    b_i[l]:=tan_b/(1+h);
    Q:=Q+(2*l+1)*(a_r[l]+b_r[l]);
   end;
  Q:=2*Q/(q1*q1);
 end;
```

- Procedure that computes the scattering functions and intensities.

```
procedure S_calc(q1,q3,theta: real);
 var
  l                        : integer;
  z,f                      : real;
 begin
  {
    Calculation of the amplitude functions
    see Van de Hulst, sec. 9.31
  }
  z:=cos(theta);
  pie_tau_calc(z);
  ab_calc(q1,q3);
  S1_r:=0; S1_i:=0;
  S2_r:=0; S2_i:=0;
  for l:=l_max downto 1 do
   begin
    f:=(2*l+1)/(l*(l+1));
    S1_r:=S1_r+f*(a_r[l]*pie[l]+b_r[l]*tau[l]);
    S1_i:=S1_i+f*(a_i[l]*pie[l]+b_i[l]*tau[l]);
    S2_r:=S2_r+f*(b_r[l]*pie[l]+a_r[l]*tau[l]);
    S2_i:=S2_i+f*(b_i[l]*pie[l]+a_i[l]*tau[l]);
   end;
  I1:=S1_r*S1_r+S1_i*S1_i;
  I2:=S2_r*S2_r+S2_i*S2_i;
 end;
```

Exercises

4.1 Consider an emulsion where equally sized droplets of the one fluid, dielectric constant ϵ_0, are suspended in another fluid of dielectric constant ϵ_1. Use the Clausius-Mossotti relation (1.22) and the expression (4.1) for the polarizability of the droplets to derive an expression for the dielectric permittivity ϵ of a suspension with volume fraction φ.

4.2 Show that for small w the form factor (4.19) expands as

$$P(\theta)_{\theta\to 0} = 1 - \frac{q^2 R_g^2}{3} \tag{4.24}$$

This leads to a possibility to measure the radius of gyration of a polymer by plotting P versus q^2, the socalled *Guinier plot*.